Improvement of the solubility and intestinal absorption of curcumin by *N*-acyl taurates and cyclodextrins

Ph.D. Dissertation

Xinpeng Li

Department of Biopharmaceutics
Kyoto Pharmaceutical University

Kyoto
2017

Table of Contents

Table of Tables

Table of Figures

List of Abbreviations

ALT	Alanine transaminase
AST	Aspartate transaminase
AUC	Area under the plasma drug concentration-time curve
BBMV	Brush border membrane vesicle
BSA	Bovine serum albumin
BUN	Blood urea nitrogen
Caco-2	Colon adenocarcinoma-2
CDs	Cyclodextrins
CF	5(6)-Carboxyfluorescein
C_{max}	Maximum plasma drug concentration
CMC	Critical micelle concentration
CMT	Sodium methyl cocoyl taurate
CUR	Curcumin
DMEM	Dulbecco's Modified Eagle Medium
DNS-Cl	Dansyl chloride
DPH	1,6-Diphenyl-1,3,5-hexatriene
EDTA	Ethylenediaminetetraacetic acid
EGTA	Ethylene glycol tetraacetic acid
ErA	Absorption enhancement ratio
Ers	Solubility enhancement ratio
FBS	Fetal bovine serum
FD4	Fluorescein isothiocyanate-labeled dextrans with average molecular weights of 4000
FD10	Fluorescein isothiocyanate-labeled dextrans with average molecular weights of 10000
HBSS	Hank's balanced salt solution
HEPES	2-[4-(2-Hydroxyethyl)-1-piperazinyl]ethane sulfonic acid
HPLC	High-performance liquid chromatography
LDH	Lactate dehydrogenase
LMT	Sodium methyl lauroyl taurate
MC	Methylcellulose

MMT	Sodium methyl myristoyl taurate
NATs	*N*-Acyl taurates
P_{app}	Apparent permeability coefficient
PBS	Phosphate buffered saline
P-gp	P-glycoprotein
PMT	Sodium methyl palmitoyl taurate
PVDF	Polyvinylidene difluoride
S.E.	Standar error
SMT	Sodium methyl stearoyl taurate
TBST	Tris-buffered saline and Tween 20
TEER	Transepithelial electrical resistance
tma-DPH	1-(4-(Trimethylamino) phenyl)-6-phenylhexa-1,3,5-hexatriene-p-toluenesulfonate
T_{max}	Time to the maximum plasma drug concentration
Tris	Tris(hydroxymethyl)amino methane
TX100	Triton X-100

Abstract

Curcumin is a polyphenolic compound named as (1E,6E)-1,7-bis(4-hydroxy-3-methoxyphenyl)hepta-1,6-diene-3,5-dione; CAS number: 458-37-7. The molecular formula is $C_{21}H_{20}O_6$ and it has a molecular weight of 368 g/mol. This compound is derived from *Curcuma longa* L. and has demonstrated versatile pharmacological effects including anti-inflammatory and antioxidant actions in extensive preclinical studies. In addition, the therapeutic effects, such as anti-tumors, were studied in human clinical trials over the last few decades. In terms of the high dose at 12 g per day in healthy volunteers, curcumin was well tolerated in the oral administration and appeared to be safe for the clinical use. However, based on the poor aqueous solubility and low intestinal permeability of curcumin, the natural product is classified as a biological classification system (BCS) Class IV molecule. The hydrolytic and light-sensitive properties also cause the rapid degradation of this natural polyphenol. Due to these characteristics, curcumin showed a low concentration in plasma after oral administration resulting in a poor bioavailability. Various approaches have been developed to overcome the bioavailability problem, such as nanoformulations. Because many ingredients in formulae are used for both solubilizers and permeation enhancers, it is of interest to investigate their multiple functions with respect to drug absorption. In our recent research, amorphous solid particles of curcumin showed an enhanced permeation across the absorptive membrane, while it was not observed in the presence of crystalline particles or supersaturated solution. Consequently, since the crystalline powder is more stable than the amorphous particles in dosage forms, the present study was focused on the development of new curcumin formulations using crystalline particles with absorption enhancers and examined their absorption-enhancing mechanisms.

Chapter I Improvement of the solubility and intestinal absorption of curcumin by *N*-acyl taurates (NATs)

NATs are a subset of acylated amino acids which are surfactants with natural lipid-like structures that exhibit amphiphilic properties. In this chapter, the effects of NATs on the small intestinal absorption of curcumin were examined in rats by an *in situ* closed-loop method. Among these NATs, 1% (v/v) sodium methyl lauroyl taurate (LMT) and sodium methyl cocoyl taurate (CMT) were the most effective in increasing the solubility and intestinal absorption of curcumin. The intestinal membrane toxicity of NATs was also evaluated by measuring the activity of lactate dehydrogenase (LDH), a cytotoxicity marker. All of them did not increase the activity of LDH in the luminal fluid, suggesting that they may be safely administered orally. The relationship between the solubility and absorption demonstrated that the drug solubility is an important factor contributing to the absorption of curcumin. However, the drug absorption was not changed when the solubility was higher than 5 μg/mL, which means that the rate-limiting step was shifted from the apparent solubility of curcumin to the permeation across the intestinal membrane. Thus, the absorption-enhancing mechanism was elucidated in the paracellular pathway using Caco-2 cells. In cellular transport studies, LMT and CMT reduced the transepithelial electrical resistance (TEER) values of Caco-2 cells and increased the transport of 5(6)-carboxyfluorescein (CF) and curcumin. Hence, besides the increased solubility, the improved permeability of curcumin by LMT and CMT also contributed to the intestinal absorption.

Chapter II Improvement of the solubility and intestinal absorption of curcumin by cyclodextrins (CDs)

CDs are a unique type of macrocyclic carriers widely used in pharmaceutical formulations owing to their versatile functions as the solubilization, stabilization, and permeation

enhancement. In this chapter, α-CD, β-CD, γ-CD, hydroxypropyl (HP)-β-CD, and dimethyl (DM)-β-CD were applied to the formulation of curcumin. The interaction between curcumin and CD molecules was investigated by phase-solubility diagrams, suggesting that 1:1 complex formation was observed in the solution except for γ-CD. The effects of various CDs on the intestinal absorption of curcumin were evaluated in rat intestine by the *in situ* closed-loop experiment. Among the tested CDs, 50 mM α-CD significantly enhanced the intestinal absorption of curcumin without causing any serious toxicity to tissues like intestinal membrane, liver, and kidney. In addition to curcumin, 50 mM α-CD increased the intestinal absorption of hydrophilic drugs including CF, fluorescein isothiocyanate-labeled dextrans with average molecular weights of 4000 (FD4), FD10, and salmon calcitonin, suggesting a molecular weight dependency of the absorption-enhancing ability. The analysis of cellular transport across Caco-2 cell monolayers showed that 50 mM α-CD reduced the TEER value of cell monolayers and improved the paracellular permeability of CF. Furthermore, in the western blotting analysis, α-CD decreased the expression of claudin-4, a tight junction-associated protein, in brush border membrane. Additionally, α-CD increased the membrane fluidity of lipid bilayers in brush border membrane vesicles and may also promote the permeation of drug molecules via the transcellular pathway. Upon these results, it is concluded that 50 mM α-CD is the optimal CD formulation to enhance the absorption not only by solubilizing curcumin but also by assisting its permeation across the intestinal membrane.

Summary

When the solubility was higher than 5 μg/mL, the rate-limiting step of curcumin absorption was shifted from the apparent drug solubility to the permeation across the intestinal membrane, which confirmed the drawbacks of curcumin in both solubility and permeability. Of tested absorption enhancers, 1% (v/v) LMT or CMT, and 50 mM α-CD significantly improved the

absorption of curcumin from the rat small intestine without inducing any serious toxicity to intestinal tissue or organs. The absorption-enhancing effect of these materials on the paracellular pathway was evidenced by Caco-2 cell model. In particular, α-CD altered the barrier properties of both the paracellular and transcellular pathways. Therefore, the intestinal absorption enhancement by absorption enhancers might be attributed to the synergistic effect of increased solubility and permeability of curcumin in their presence.

Introduction

Curcuma longa L. is a medicinal plant of the ginger family which has been used for many centuries in India, China, and South East Asia. As claimed in the traditional medicine, it has therapeutic effects to various diseases, such as biliary disorders, anorexia, coryza, cough, diabetic wounds, hepatic disorder, rheumatism, sinusitis, abdominal pains, sprains, and swellings caused by injury.[1)] As the major component, curcumin (CUR) has demonstrated versatile pharmacological effects in extensive animal models where it worked as anti-inflammatory, antioxidant, anticarcinogen, antimicrobial, hepatoprotective, thrombosuppressive, cardiovascular, hypoglycemic, and antiarthritic agents. It also exhibited biological activities to Alzheimer's diseases, cataract formation, pulmonary toxicity and fibrosis, psoriasis, and renal ischemia.[2,3)] The underlying mechanisms of the treatment may be due to the modulation of immune responses by CUR through its direct actions on signal pathways or target gene expression.[4,5)] Furthermore, the therapeutic activities of CUR have been evaluated in human clinical trials which revealed the potential actions to tumors and psoriasis vulgaris.[6,7)] In terms of the high dose at 12 g per day used in healthy volunteers, CUR was well tolerated in the oral administration and appeared to be safe for the clinical use.[8)]

CUR is a polyphenolic compound characterized in Table 1. Due to these characteristics, CUR appears to be a low concentration in plasma after oral administration, resulting in a poor bioavailability.[9)] To achieve much more therapeutic effects, various approaches have been developed by many scientists in the world, such as co-administration of CUR with inhibitors of glucuronidation or prodrugs by conjugation.[10-12)] In current days, CUR nanoformulations have attracted great attention including liposomes, solid lipid nanoparticles, niosomes, polymeric nanoparticles, polymeric micelles, cyclodextrins, dendrimers, silver and gold nanoparticles. Most of these nanoformulations were attempted to solubilize CUR and increase its stability in

aqueous solutions. Nevertheless, because many ingredients in formulae are used for both solubilizers and permeation enhancers, it is of interest to investigate their multiple functions with respect to drug absorption.

Recently, we developed a novel strategy for improving the bioavailability of CUR by amorphous solid particles.[13] It is found that these drug particles enhanced the permeation across the absorptive membrane which was not observed in the presence of crystalline CUR powder or supersaturated solution. Consequently, since the crystalline powder is more stable than the amorphous particles in dosage forms, the present study was focused on the development of new curcumin formulations using crystalline particles with absorption enhancers and examined their absorption-enhancing mechanisms.

Up to date, more than 200 intestinal absorption enhancers have been published in previous preclinical studies, some of which also have been undergoing the investigation in the clinical trials.[14,15] Over the past few decades, our research has been demonstrating several promising absorption enhancers including surfactants, protease inhibitors, NO donors, and polymers, which showed a strong absorption-enhancing efficacy and a low local toxicity in animal or cell studies. Of various surfactants, bile salts, sodium glycocholate and sodium taurocholate, and alkylsaccharide, *N*-lauryl-β-D-maltopyranoside increased the intestinal absorption of poorly absorbed drugs including 5(6)-carboxyfluorescein (CF), phenol red, human calcitonin, ebiratide, enkephalin analogs, and insulin.[16-23] As a new type absorption enhancer, Gemini surfactant, sodium dilauramidoglutamide lysine also exhibited the intestinal absorption-enhancing effects on small hydrophilic molecules and macromolecules like protein and peptide drugs.[24] In addition, other types of surfactants, including sucrose fatty acids esters, *N*-acyl amino acids, and *N*-acyl taurates improved the poor absorption of alendronate from the intestine.[25,26] With respect to protease inhibitors, bacitracin promoted the intestinal absorption of peptide and protein drugs by improving drug stability against the peptidases in the intestinal regions.[27-29]

In comparison to the conventional absorption enhancers, NO donors were able to enhance the absorption of CF without any regional difference in the intestine.[30] In terms of polymers, polyamidoamine (PAMAM) dendrimers improved the absorption of peptide and protein drugs either in nasal delivery or in pulmonary administration.[31,32] On the other hand, the polymers, such as polyethylene glycol 20000 and polyoxyethylene alkyl ethers worked as P-gp modulators to reverse the efflux activity produced by P-gp transporters.[33,34] As reported in these studies, most of these absorption enhancers were safe to the mucosal membrane without causing serious damages. Thus, applying absorption enhancers in formulations is still a useful strategy to enhance the intestinal absorption of poorly absorbable drugs like CUR.

In this study, the intestinal absorption of CUR was examined using an *in situ* closed-loop experiment in the presence of various absorption enhancers. To investigate the mechanisms of absorption enhancement of CUR, the factors as solubilization and permeation enhancement were evaluated when the natural product was co-administered with the absorption enhancers. Regarding the drug permeation, the cellular transport of CF, a paracellular marker, was examined in Caco-2 cell monolayers and the intestinal expression of claudin-4 was determined in brush border membrane vesicles (BBMVs) in the combination with a absorption enhancer. Furthermore, the transcellular permeation of CUR enhanced by the absorption enhancer was also evaluated in light of the membrane fluidity of BBMVs.

Table 1 Characteristics of CUR[35)]

Chemical name	(1E,6E)-1,7-bis(4-hydroxy-3-methoxyphenyl)hepta-1,6-diene-3,5-dione
C.A.S number	458-37-7
Molecular formula	$C_{21}H_{20}O_6$
Molecular weight	368 g/mol
Chemical structure	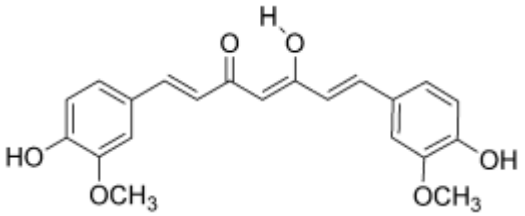 Enol form (at pH > 8) 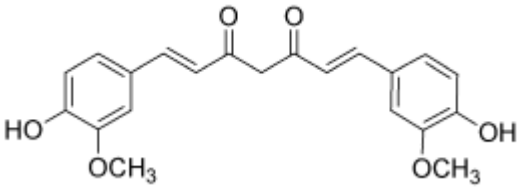 Keto form (at pH 1-7)
Physical and chemical properties	
Physical state	Solid crystalline
Color	Orange-yellow (at pH = 7)
Odor	odorless
Solubility	11 ng/mL (in water at pH 5)[36)]
Permeability	Log Kow = 3.29[a]
pK_a	7.8, 8.5 and 9.0[37)]
Light sensitivity	Light sensitive

[a]Note: Estimated using EPI Suite™ (Ver. 4.11, 2012, developed by US EPA)

Chapter I Improvement of the solubility and intestinal absorption of curcumin by *N*-acyl taurates

N-acyl taurates (NATs) are a subset of acylated amino acids which are surfactants with natural lipid-like structures that exhibit amphiphilic properties.[38] These taurates showed excellent detergency and stability over the whole pH range in aqueous solution.[39] Due to medium-chain fatty acyl moieties, NATs possess a variety of properties and may be used for different purposes. Since they were invented from 1930s, taurates are mainly used in the personal care applications. For example, sodium cocoyl taurate (CMT) were applied as the primary surfactant to replace the sodium lauryl sulphate (SLS) in the SLS free product.[40] Some taurates with long-chain fatty acids have been identified in brain, liver, kidney, and skin.[41,42] These endogenous taurates activate multiple members of the transient receptor potential (TRP) family of calcium channels, including TRPV1 and TRPV4. Because TRPV4 locates in many different epithelial cells, the activation of this channel may modulate epithelial permeability by regulating extracellular and intracellular calcium concentrations.[43] Recently, the absorption-enhancing abilities of NATs have been examined in the intestinal absorption of alendronate, which is characterized as a water-soluble and poorly absorbed drug.[26] However, the enhancing effects on other poorly absorbed drugs are still not well understood. Thus, five NATs with C8-C18 fatty acyl chains (Fig. 1) were selected to evaluate their enhancing effects on the intestinal absorption of CUR.

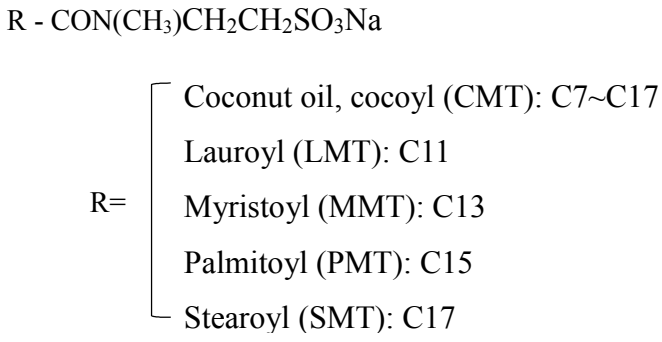

Fig. 1. Chemical structure of *N*-acyl taurates

1.1 Materials and methods

1.1.1 Materials

Curcumin, LDH-cytotoxic test Wako, albumin (from bovine serum, Cohn fraction V, pH 7.0), sodium carbonate were bought from Wako Pure Chemical Industries, Ltd. (Osaka, Japan). 5(6)-Carboxyfluorescein was produced by Eastman Kodak Company (Rochester, NY, USA). *N*-acyl taurates was supplied by Nikko Chemical Co. Ltd. (Osaka, Japan). Methylcellulose was purchased from Nacalai Tesque, Inc. (Kyoto, Japan). Caco-2 cells was provided by Dainippon Sumitomo Pharma Co., Ltd. (Osaka, Japan). Dulbecco's modified eagle's medium (DMEM), fetal bovine serum, and MEM non-essential amino acid solution was supplied by Life Technologies Corporation (Carlsbad, CA, USA). 0.25% Trypsin-1 M EDTA (ethylenediaminetetraacetic acid) and antibiotic-antimycotic mixed stock solution (10,000 U/mL penicillin, 10 mg/mL streptomycin, 25 mg/mL amphotericin B, 0.85% w/v saline) were manufactured by Dojindo Laboratories (Kumamoto, Japan). Hank's balanced salt (HBS; H6136-10X1L) was purchased from Sigma-Aldrich Chemical Co. Ltd. (St. Louis, MO, USA). Polycarbonate membrane Transwell inserts (12 wells, 12 mm in diameter, 0.4-μm pore size,

sterile) were manufactured by Corning Inc. (Corning, NY, USA). All other reagents used in the experiments were of analytical grade.

1.1.2 Solubility of CUR in 1% NAT formulations

An over-saturated CUR suspension was prepared in 1 mL 1% (v/v or w/v) NAT in PBS (pH 6.5). The suspension was agitated for 5 min at 25 °C using Vortex-Genie 2 (Scientific Industries, Inc., Bohemia, NY, USA), and then was centrifuged at 9660 × *g* for 5 min. The supernatant was collected for the assay. The solubility enhancement ratio (ErS) was calculated from the following equation:

ErS = Solubility with absorption enhancer/Solubility without absorption enhancer

1.1.3 Intestinal absorption study of CUR with NATs

The intestinal absorption was evaluated by administering CUR into rat small intestine in an *in situ* closed-loop experiment.[18,44)] All experiments were conducted in compliance with the guidelines of the Animal Ethics Committee at Kyoto Pharmaceutical University. The crystalline powder of CUR was suspended in 1% (v/v or w/v) NAT in pH 6.5 PBS containing 1% (w/v) methylcellulose (MC) to reach the concentration at 16.67 mg/mL, followed by agitation for 5 min at 25 °C, ahead of the intestinal administration. The drug suspension without any NAT was set as the control. Prior to the experiment, male Wistar rats, weighing 220-260 g, were fasted for 16 h with a free access to water. To begin the experiment, the animals were anesthetized by intraperitoneal injection of sodium pentobarbital (32 mg/kg body weight) and placed under a heating lamp to keep warm. The small intestine was exposed through a midline abdominal

incision. After ligating the bile duct, polyethylene cannulas were inserted into the incisions of the small intestine at duodenal and ileal ends. The small intestine was then washed with PBS (10 mL × 2) to clean the intestinal content. Three milliliters of the drug suspension was administered into the small intestine and then the cannulas were closed by forceps.[45] Blood samples (~ 0.4 mL) were withdrawn from the jugular vein at the predetermined time up to 240 min after administration. 150 μL of plasma was separated immediately by centrifugation at 9660 × *g* for 5 min and stored at -30 °C until assay.

The maximal plasma concentration of CUR (C_{max}) and the time to maximal plasma concentration (T_{max}) were read from the plasma drug concentration-time curve. The area under the curve (AUC) between 0 and 240 min was calculated manually by the trapezoidal method. The absorption enhancement ratio (ErA) was obtained from the following equation:

$$ErA = AUC_{0\rightarrow 240\ min}\ \text{with absorption enhancer} / AUC_{0\rightarrow 240\ min}\ \text{without absorption enhancer}$$

1.1.4 Intestinal membrane toxicity after administration of NATs

The intestinal membrane toxicity of NATs was evaluated in terms of the activity of LDH released from intestinal epithelia cells. PBS (pH 6.5), 1% NAT, and 3% (v/v) Triton X-100 (TX100) were administered, respectively, into the small intestinal loops of experimental animals by the *in situ* closed-loop method. After 240 min post administration, the small intestine was washed with 30 mL of ice-cold PBS (pH 7.4) which was collected from the ileal end and stored in an ice box subsequently. The washing solution was centrifuged at 200 × *g* for 7 min at 4 °C to get rid of any deposition, and then was diluted by 100 times. The activity of LDH was determined by mixing the dilution with LDH-cytotoxicity test Wako kit and reading the

absorbance at 590 nm with a microplate multi-detection reader (Synergy HT with Gen 5 software; BioTek Instruments, Inc., Winooski, VT, USA).

1.1.5 Cellular transport of CF and CUR with NATs

1.1.5.1 Cell culture

Caco-2 cells were cultured in DMEM containing 10% (v/v) FBS, 1% (v/v) antibiotic-antimycotic mixed stock solution, and 0.1 mM MEM non-essential amino acid solution in a filter cap cell culture flask with a humidified atmosphere of 5% CO_2 at 37 °C.[28,29] Cells at passage 54-68 were seeded onto 12-well plates fitted with polycarbonate inserts at a density of 1×10^5 cells/well. The cultivated cells grew for 21 days by changing the culture medium every 2 days. Transepithelial electrical resistance (TEER) values of the cell monolayers were measured using a Millicell-ERS voltohmmeter (EMD Millipore Corporation, MA, USA). When these values were more than 500 ohms·cm^2, Caco-2 cell monolayers were used for the following experiments.

1.1.5.2 Cellular transport study of CF

Cellular transport was studied from the apical and basolateral direction by adding a donor solution/suspension to the apical compartment. Generally, the pH value in the apical side of jejunum is about 6.5, while the pH of the basolateral side is about 7.4. Thus, in the present study, a similar pH gradient was used to mimic the physiological condition of the small intestine.

After 1 h incubation in HBSS at 37 °C, the transport experiments were initiated by replacing with 0.5 mL of 10 μM CF in HBSS (pH 6.5) in the apical side. At the defined times up to 360

min, the TEER value was measured and 200 μL sample was taken out from 1.5 mL of the receiving HBSS (pH 7.4) which was then supplemented by the fresh medium. The fluorescence intensity of CF was measured at an excitation wavelength of 485 and emission wavelength of 528 nm using a microplate multi-detection reader.

1.1.5.3 Cellular transport study of CUR

In the transport experiments of CUR, 0.5 mL of 2 mM drug suspension, with or without NAT, in HBSS (pH 6.5) was added to the apical side of 1 h-incubated Caco-2 cell monolayers. 1.5 mL of HBSS (pH 7.4) containing 5% (w/v) bovine serum albumin (BSA) was applied in the basolateral compartment. Other procedures were kept same as the cellular transport of CF in1.1.5.2. The samples were stored at -30 °C until assay.

1.1.5.4 Apparent permeability coefficient (P_{app})

Based on the transported compound in the receiving solution, the P_{app} value was calculated as follows:

$$P_{app} = (dQ/dt)/(A \cdot C_0)$$

where P_{app} is the apparent parameter of permeability (cm/s), dQ/dt is the rate of the test compound appearance in the receiver side (pmol/s), A is the membrane surface area (1.12 cm^2), and C_0 is the initial concentration or solubility of the test compound in donor solution or suspension (nM).

1.1.6 Determination of CUR by HPLC

The assay of CUR in the solubility and intestinal absorption studies was determined using an HPLC system configured with a binary pump (LC-20AB; Shimadzu Corporation, Kyoto, Japan) and UV/Vis detector (SPD-20A). CUR was eluted at 35 °C by a C18 reverse-phase column (150 × 4.6 mm, 5C18-AR-II; Nacalai Tesque Co. Ltd, Kyoto, Japan) and was analyzed at 420 nm. The mobile phase was a mixture of 5% (v/v) acetic acid and methanol (32:68, v/v) with a flow of 1 mL/min. In order to determine the concentration of CUR in plasma, 150 μL plasma sample was mixed with 15 μL 5% (v/v) acetic acid. CUR was extracted from the treated plasma by 1 mL ethyl acetate, which was then evaporated at 40 °C for 30 min and re-dissolved by 150 μL methanol. 50 μL of the resulting sample was injected into the HPLC system.

The concentration of CUR in the cellular transport study was measured in the same HPLC system as described above, while the detector was replaced with a fluorescence detector (RF-10AXL; Shimadzu Corporation, Kyoto, Japan). The excitation and emission wavelengths were set at 420 and 530 nm, respectively.[46] 150 μL of receiving solution was mixed with 15 μL 5% (v/v) acetic acid. The BSA in the sample was precipitated by mixing the treated sample with 335 μL of methanol, followed by centrifuging at 9660 × *g* for 10 min. The supernatant was collected for HPLC injection.

1.1.7 Statistical Analyses

Results are expressed as the mean ± S.E. of at least three experiments. Tests of statistical significance of different experimental groups were performed using Dunnett's test, in which p

< 0.05 was considered significant. Significance levels are denoted as (n.s.) not significantly different, (*) $p < 0.05$, (**) $p < 0.01$, and (***) $p < 0.001$.

1.2 Results and discussion

1.2.1 Solubility of CUR improved by NATs

In order to improve the free drug in the aqueous solution, CUR was suspended in 1% NAT solution by an agitation method. Compared to the control, the solubility of CUR was improved with an ErS at more than 90 by all NATs, especially CMT and LMT (Table 2). The rank order of the solubilizing effect was CMT > LMT > MMT > SMT > PMT.

As a subset of acylated amino acids, NATs are used as solubilizers in the solution for hydrophobic substances. NATs with short fatty acid chains, such as C8-C12, could improve the solubility of CUR effectively and the solubilizing effects of these taurates decreased along with the increase in the length of their fatty acid chains. The strong solubilizing effect of LMT may be ascribed to the formed micelles when the applied concentration was above CMC which was about 0.3% (w/v).[47] Similarly because LMT is the main composition of CMT, it is possible that CUR molecules were entrapped in the micelles in CMT solution. Moreover, the mixed micelles formed by complex compositions in CMT might contribute to the highest solubility of CUR.

Table 2 Solubility of CUR in the presence of 1% NATs

Group	Solubility (μg/mL)	ErS
CUR	0.007 ± 0.001	1
+1% (v/v) CMT	35 ± 0.34***	5000
+1% (v/v) LMT	29 ± 0.69***	4143
+1% (w/v) MMT	5.7 ± 0.88***	814
+1% (w/v) PMT	0.63 ± 0.14	90
+1% (w/v) SMT	0.73 ± 0.10	104

Results are expressed as the mean ± S.E. of at least 3 experiments.

(***) $p<0.001$, compared with CUR (control). (Table 2 in *Biol. Pharm. Bull.* **2017**, *40* (12), 2175–2182.)

1.2.2 Intestinal absorption of CUR in the presence of NATs

The intestinal absorption of CUR in the presence of 1% NATs was studied by administering the drug suspension into the loop of the rat small intestine. As shown in Fig. 2, the plasma CUR appeared obviously in the first hour after administering CUR with CMT, LMT, or MMT. The concentration of CUR in plasma increased slowly in the experiment using SMT as the absorption enhancer, while the PMT group presented a similar profile to the control. The pharmacokinetic parameters in Table 3 showed a significant increase in the intestinal absorption of CUR in the presence of CMT, LMT, and MMT. Based on the ErA values, the rank order of the absorption-enhancing ability is as follows: LMT ≥ MMT ≥ CMT > SMT > PMT. Furthermore, the bioavailability and absorption rate of CUR were estimated in Table 4 by a deconvolution method.[48] In the presence of CMT, LMT, and MMT, after 240 min treatment, the drug bioavailability (F) could reach above 17%. Furthermore, both CMT and LMT groups

display the fastest absorption rate of CUR at 1.24 (ng/min), suggesting that these two taurates have a fast onset of absorption-enhancing action. In contrast, SMT displayed a mild effect on the absorption of CUR in the small intestine. However, it was difficult to estimate these parameters in the control and PMT groups owing to the low drug absorption.

In light of the solubilizing ability of NATs, one possible explanation to the enhanced absorption might be the *N*-acyl taurate micelles which can act as a drug reservoir to maintain a constant free CUR for the intestinal absorption. It also should be noted that the drug suspension consisted of free CUR, CUR in micelles, and the solid drug particles.[49] In this case, the dissolution rate of solid CUR was accelerated by absorption enhancers. Therefore, the relationship between the solubility and absorption was investigated when CUR was co-administrated intestinally with NATs. As shown in Fig. 3, a good sigmoidal relationship (R=0.8725) was obtained between two indexes, demonstrating that the solubility is an important factor contributing to the absorption of CUR in the presence of NATs. However, the drug absorption was not changed when the solubility was higher than 5 μg/mL. This finding indicates that the rate-limiting step was shifted from the apparent solubility of CUR in micelles to the permeation across the intestinal membrane. Therefore, it was regarded that NATs, especially LMT and CMT, acted as both solubilizer and permeation enhancer to promote the absorption of CUR in the small intestine.

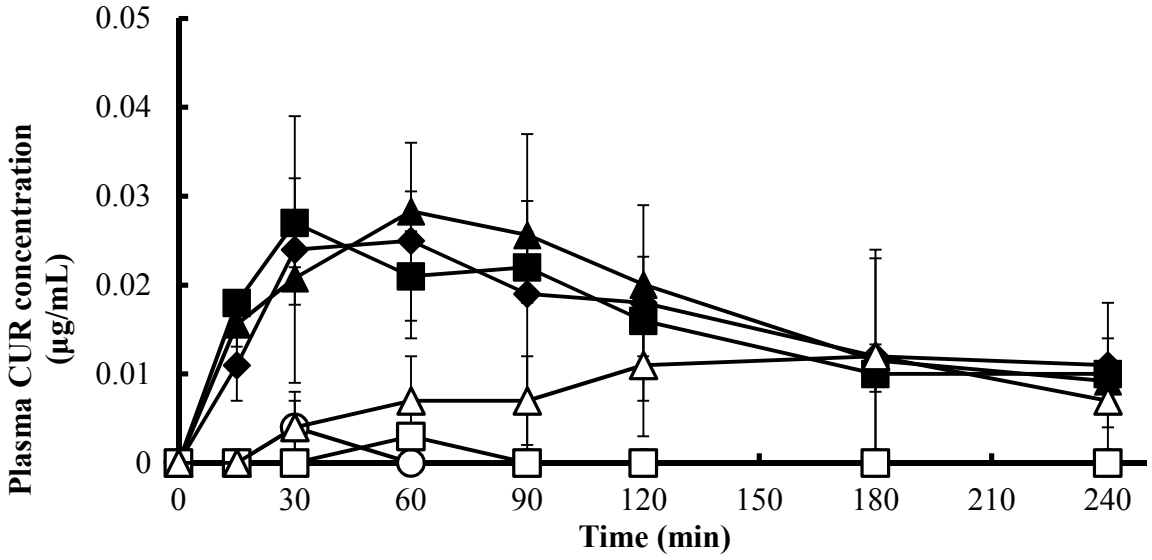

Fig. 2. Absorption of CUR (200 mg/kg) from rat small intestines in the presence of 1% NATs

Keys: (○) CUR only, (▲) +1% (v/v) LMT, (■) +1% (v/v) CMT, (♦) +1% (w/v) MMT, (□) +1% (w/v) PMT, (△) +1% (w/v) SMT. Results are expressed as the mean ± S.E. of 3-4 experiments. (Fig. 2 in *Biol. Pharm. Bull.* **2017**, *40* (12), 2175–2182)

Table 3 Pharmacokinetic parameters of CUR in the presence of 1% NATs after intestinal administration to rats

Group	C_{max} (μg/mL)	T_{max} (min)	$AUC_{0\rightarrow240\ min}$ (μg/mL·min)	ErA
CUR	0.004 ± 0.004	30 ± 0	0.090 ± 0.090	1
+1% (v/v) CMT	0.027 ± 0.005	30 ± 0	3.8 ± 0.68*	42
+1% (v/v) LMT	0.016 ± 0.007	27 ± 12	4.2 ± 0.34**	47
+1% (w/v) MMT	0.037 ± 0.007	60 ± 17	3.9 ± 1.1*	43
+1% (w/v) PMT	0.003 ± 0.001	60 ± 0	0.10 ± 0.020	1
+1% (w/v) SMT	0.020 ± 0.001	150 ± 24	1.9 ± 1.6	21

Results are expressed as the mean ± S.E. of 3-4 experiments. (**) $p< 0.01$, (*) $p< 0.05$, compared with CUR (control). (Table 1 in *Biol. Pharm. Bull.* **2017**, *40* (12), 2175–2182)

Table 4 Estimation of bioavailability and absorption rate of CUR using a deconvolution method

Time (min)	+1% (v/v) CMT		+1% (v/v) LMT		+1% (w/v) MMT		+1% (w/v) SMT	
	F (%)	Absorption rate (ng/min)	F (%)	Absorption rate (ng/min)	F (%)	Absorption rate (ng/min)	F (%)	Absorption rate (ng/min)
15	0.9	0.60	0.8	0.53	0.6	0.40	0.2	0.14
30	2.7	1.24	2.3	0.98	2.1	1.01	0.5	0.19
60	6.1	1.11	6.0	1.23	5.7	1.20	1.4	0.28
90	9.1	0.99	9.7	1.24	8.6	0.97	2.4	0.33
120	11.4	0.80	12.6	0.98	11.1	0.81	3.7	0.44
180	14.9	0.58	16.4	0.62	14.8	0.62	6.9	0.53
240	17.7	0.46	18.9	0.42	17.7	0.49	9.2	0.39

Note: Bioavailability (F) was estimated based on the ratio of $AUC_{0\text{-}240\ min}$ from the intestine to that of intravenous injection.

(Reported data in *Biol. Pharm. Bull.* **2017**, *40* (12), 2175–2182

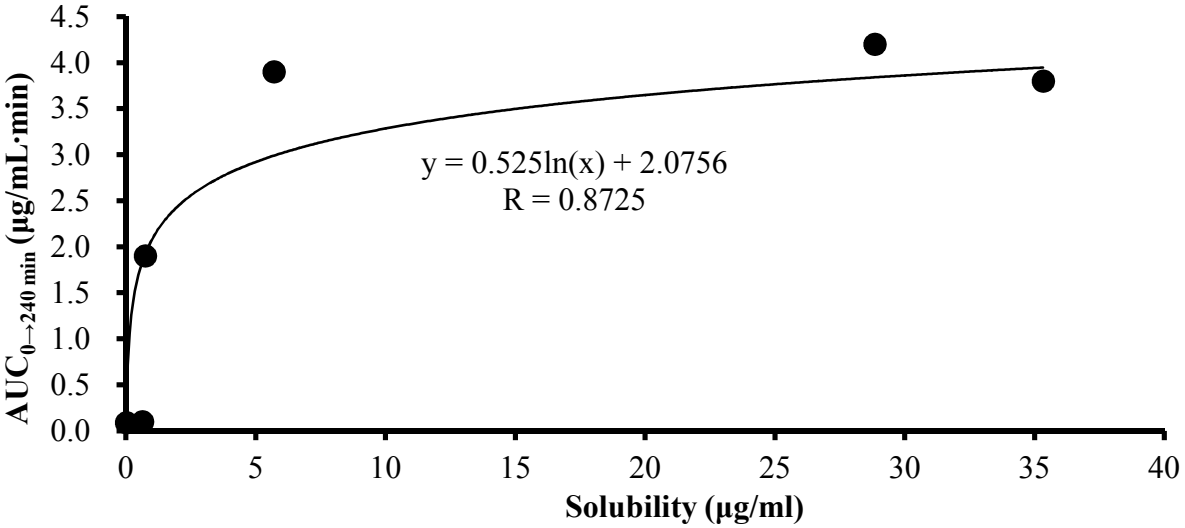

Fig. 3. The relationship between the solubility and intestinal absorption of CUR in the presence of 1% NATs

(Fig. 7 in *Biol. Pharm. Bull.* **2017**, *40* (12), 2175–2182)

1.2.3 Intestinal membrane toxicity in the presence of NATs

The activity of LDH released from the rat small intestine was determined in the intestinal washing solution after 4 h treatment of 1% NAT. The results in Fig. 4 presented that none of the tested NATs induced the remarkable release of LDH. On the contrary, 3% (v/v) TX100, the positive control, increased the activity of LDH in the intestinal washing solution. This means that NATs did not cause serious damage and irritation to the mucosal membrane of rat intestine.

LDH is a cytosolic enzyme which was recommended as a potential marker for the evaluation of intestinal damage.[50] Some attention should be paid to the depletion of LDH in the tissue since the LDH release was less in LMT group than that in the control. Nevertheless, it is found that this depletion would not occur in the taurate groups on the basis of the considerably high LDH activity in TX100 treated group. Consequently, the exact reason for the decrease of LDH is still not clear in the present study.

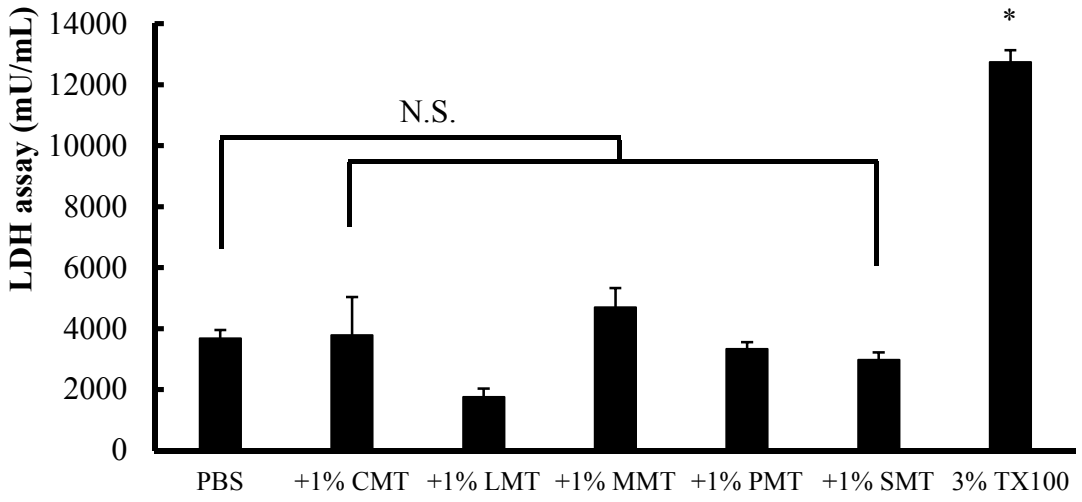

Fig. 4. The activity of LDH released from the intestinal membrane in the presence of 1% NATs

Results are expressed as the mean ± S.E. of 3-4 experiments. N.S. means no significant difference compared with PBS (control). (*) $p < 0.05$, compared to PBS. (Fig. 3 in *Biol. Pharm. Bull.* **2017**, *40* (12), 2175–2182)

1.2.4 Effects of NATs on the permeation of poorly absorbable drugs across Caco-2 cell monolayers

1.2.4.1 TEER values of Caco-2 cell monolayers

To evaluate the barrier function of Caco-2 cell monolayers, the TEER value was monitored for 6 h in the cellular transport study. As depicted in Fig. 5, the cellular TEER value changed in the NAT concentration-dependent manner when Caco-2 cells were exposed to 0.003-0.1% (v/v) of either CMT or LMT. The TEER values decreased to a steady state in the presence of the high concentration of both taurate solutions. In addition, at the concentration of 0.01%,

CMT produced a stronger efficacy than LMT on the barrier of Caco-2 cells and induced a reversible change of TEER value. Thus, the substantial decrease of TEER values indicates that high concentrations of both CMT and LMT could disrupt tight junctions in the paracellular pathway.

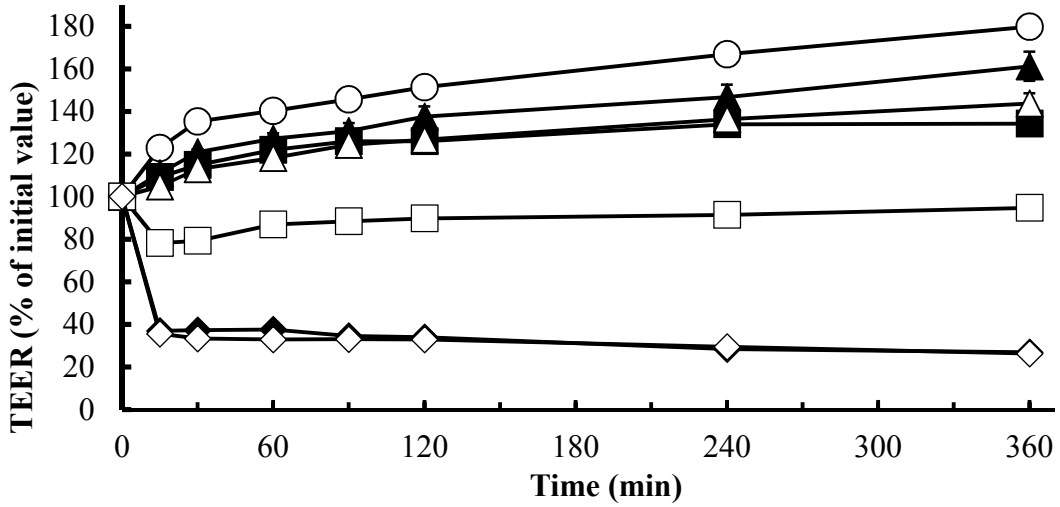

Fig. 5. TEER changes of Caco-2 cell monolayers in the presence of CMT and LMT

Keys: (○) CF, (▲) +0.003% (v/v) LMT, (■) +0.01% (v/v) LMT, (♦) +0.1% (v/v) LMT, (△) +0.003% (v/v) CMT, (□) +0.01% (v/v) CMT, (◊) +0.1% (v/v) CMT. Results are expressed as the mean ± S.E. of 3 experiments. Some error bars of S.E. are within the size of symbols.

(Fig. 4 in *Biol. Pharm. Bull.* **2017**, *40* (12), 2175–2182)

1.2.4.2 Effects of CMT and LMT on the cellular transport of CF

The effects of CMT and LMT on the paracellular permeation across the intestinal epithelia were studied in the cellular model of Caco-2 using CF as a paracellular marker. As shown in Fig. 6, the P_{app} value was improved from $(0.13 \pm 0.01) \times 10^{-6}$ cm/s in the control to $(12.58 \pm 0.73) \times 10^{-6}$ and $(11.61 \pm 0.21) \times 10^{-6}$ cm/s in 0.1% CMT and LMT solution, respectively. On

the contrary, the taurate solutions at other concentration did not change the permeability of CF significantly. In accordance with the fast recovery observed in TEER value, 0.01% CMT just accelerated the permeability 3-fold higher than the control.

The enhanced permeability of CF in this experiment further suggested that both CMT and LMT had a positive effect on the reduction of the paracellular barrier in the intestine, so that they could improve the intestinal absorption. This effect was linked to their applied concentrations in the solution. Additionally, this result is consistent with our previous work where CMT effectively improved the intestinal absorption of alendronate, a poorly absorbed drug in the oral administration. Hence, it is assumed that these two taurates would enhance the intestinal absorption of poorly absorbable drugs with similar molecular size to CF (MW=376) via the paracellular pathway.

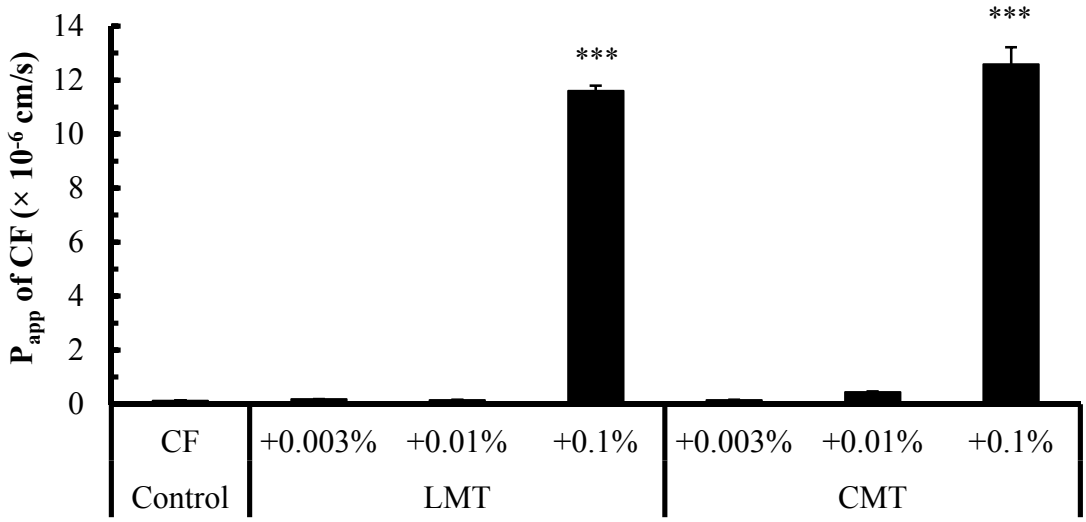

Fig. 6. Cellular transport of CF in the presence of either CMT or LMT

Results are expressed as the mean ± S.E. of 3 experiments. (***) $p< 0.001$, compared with control. (Fig. 5 in *Biol. Pharm. Bull.* **2017**, *40* (12), 2175–2182)

1.2.4.3 Effects of CMT and LMT on the cellular transport of CUR

To examine the effects of CMT and LMT on the permeability of CUR, CUR suspension containing each NAT was applied as the donor in Caco-2 cell models. As is evident in Fig. 7, the permeability of CUR across cellular layers was markedly improved by 0.1% CMT or LMT. The P_{app} value increased from $(0.70 \pm 0.04) \times 10^{-6}$ cm/s in free CUR suspension to $(5.36 \pm 0.60) \times 10^{-6}$ and $(6.74 \pm 0.38) \times 10^{-6}$ cm/s in CMT and LMT solution, respectively.

Given the drug permeation was the rate-limiting step, the enhanced absorption of CUR in the small intestine might be attributed to the improved paracellular permeation induced by these taurates. In our previous study, it has been proved that *N*-acyl amino acid was able to improve the paracellular permeation of drugs by loosening the tight junctions through the regulation of the expression of tight junction-associated proteins. Therefore, it is plausible that CMT and LMT could enhance the diffusion of free CUR across the intestinal membrane by the similar mechanism.

Furthermore, based on our previous study, *N*-acyl amino acid increased the drug permeation through a transcellular pathway by increasing the plasma membrane fluidity of epithelial cells.[26] In this case, CMT and LMT may act to enhance the intestinal absorption of CUR in the same way. Therefore, more evidence regarding the transcellular permeation is needed in the future.

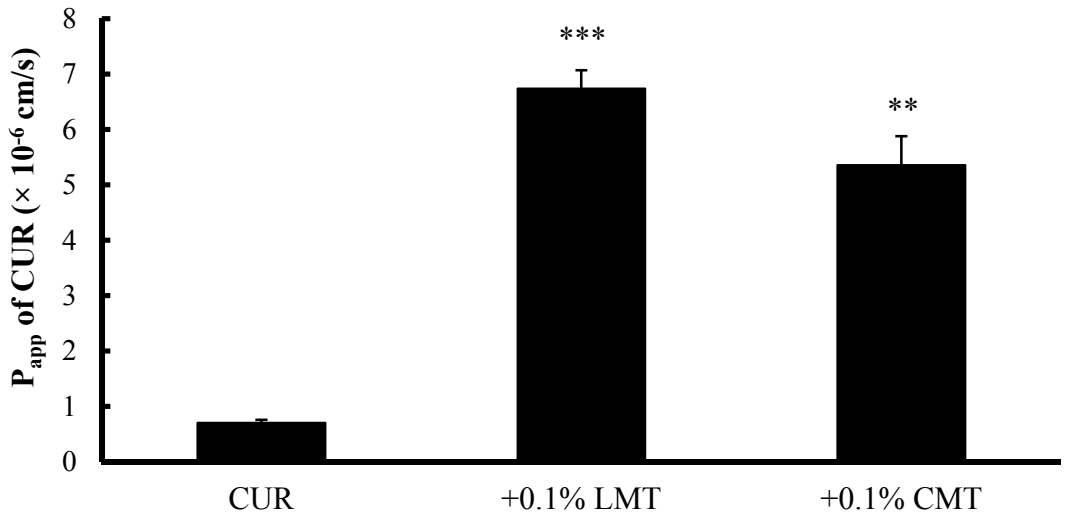

Fig. 7. Cellular transport of CUR in the presence of either CMT or LMT

Results are expressed as the mean ± S.E. of 3 experiments. (***) p< 0.001, compared with control. (Fig. 6 in *Biol. Pharm. Bull.* **2017**, *40* (12), 2175–2182)

1.3 Conclusions

In this chapter, NATs were used as solubilizers and absorption enhancers to improve the intestinal absorption of CUR. Of these taurates, CMT and LMT were the superior types which not only improved the aqueous solubility of CUR but also enhanced the drug absorption in rat small intestines. The activity of LDH released from the intestinal membrane demonstrated that all tested NATs were potentially safe excipients without causing serious damage and irritation to the intestinal tissue. The cellular transport of CF indicated that CMT and LMT were able to enhance the paracellular permeation by disrupting the barrier of cellular layers. In the same Caco-2 cell model, the permeability of CUR enhanced by both taurates was verified in terms of significantly increased P_{app} values. These results suggested that co-administration with either CMT or LMT would be a simple and effective method to enhance the absorption of CUR in the small intestine by improving the drug solubility and permeability simultaneously.

Chapter II Improvement of the solubility and intestinal absorption of curcumin by cyclodextrins

CDs are made of 6-8 units of oligosaccharides which form a non-polar cavity in the center. They are a unique type of macrocyclic carriers widely used in pharmaceutical formulations owing to their versatile functions as the solubilization, stabilization, and permeation enhancement. In order to improve the activities, numerous CD derivatives were synthesized by adding functional moieties including hydroxypropyl and methyl groups.[36] As solubilizers, CDs were employed to overcome low water solubility of lipophilic drugs and ameliorate their absorptions by producing a high concentration gradient between drugs and various epithelial membranes. HP-β-CD was applied to increase drug bioavailability in various administrations including oral, ocular, and transdermal routes.[51-53] In addition, CDs were used as the chemical absorption enhancers to modulate the drug permeation across the epithelial membranes. It was demonstrated that the natural types of CDs could work as carriers to pass through Calu-3 layers by a passive diffusion via a paracellular pathway rather than a transcelluar pathway.[54] The methylated CDs may either enhance the paracelluar permeation of macromolecules by opening tight junctions or activate cellular uptake in the transcelluar pathway by macropinocytosis.[55,56] As reported previously, CDs are capable to improve the aqueous solubility and stability of CUR. However, few studies have been examined on the action of CDs to alter the low permeability across the mucosal membrane. Therefore, in this chapter, the effects of various CDs, α-, β-, γ-CD, HP-β-CD, and DM-β-CD (Fig. 8), on the intestinal absorption of CUR was studied, followed by the elucidation of the absorption-enhancing mechanisms.

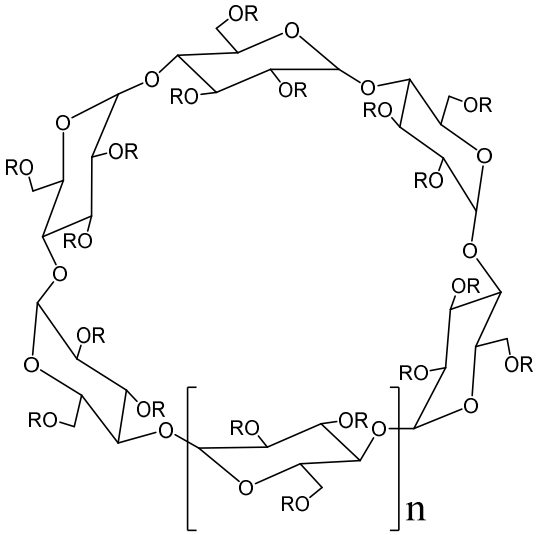

Fig. 8. Chemical structure of cyclodextrins

n=1 (α), 2 (β), 3 (γ); R=H-, $CH_3CH(OH)CH_2$-, or CH_3-

2.1 Materials and methods

2.1.1 Materials

Curcumin, salmon calcitonin, Glucose B test kit, calcium E test kit, lactate dehydrogenase (from chicken heart), coomassie brilliant blue (CBB) G-250, transaminase CII-test Wako, albumin (from bovine serum, Cohn fraction V, pH 7.0), sodium carbonate, and 1-(4-(trimethylamino) phenyl)-6-phenylhexa-1,3,5-hexatriene-p-toluenesulfonate (tma-DPH) were bought from Wako Pure Chemical Industries, Ltd. (Osaka, Japan). Insulin, 2,6-Di-O-methyl-β-CD (DM-β-CD), γ-CD, Chemi-Lumi One Ultra, and dansyl chloride (DNS-Cl) were supplied by Nacalai Tesque, Inc. (Kyoto, Japan). α-CD, β-CD, and HP-β-CD were produced by Nihon Shokuhin Kako Co., Ltd. (Tokyo, Japan). 5(6)-Carboxyfluorescein was manufactured by Eastman Kodak Company (Rochester, NY, USA). Fluorescein isothiocyanate-dextrans with average molecular weights of 4000 (FD4) and 10000 (FD10), Hank's balanced salt (H6136-10X1L), and 1,6-diphenyl-1,3,5-hexatriene (DPH) were purchased from Sigma-Aldrich Chemical Co. (St. Louis, MO, USA). Cytotoxicity detection kit was produced by Roche

Diagnostics GmbH (Penzberg, Germany). QuantiChrom™ Urea Assay Kit was supplied by BioAssay Systems, Hayward (CA, USA). Caco-2 cells were bought from Dainippon Sumitomo Pharma Co., Ltd. (Osaka, Japan). Dulbecco's modified eagle's medium (DMEM), fetal bovine serum, and MEM non-essential amino acid solution were manufactured by Life Technologies Corporation (Carlsbad, CA, USA). 0.25% Trypsin-1 M EDTA (ethylenediaminetetraacetic acid) and antibiotic-antimycotic mixed stock solution (10,000 U/mL penicillin, 10 mg/mL streptomycin, 25 mg/mL amphotericin B, 0.85% w/v saline) were prepared by Dojindo Laboratories (Kumamoto, Japan). Polycarbonate membrane Transwell inserts (12 wells, 12 mm in diameter, 0.4-μm pore size, sterile) were manufactured by Corning Inc. (Corning, NY, USA). Claudin-4 Mouse Monoclonal Antibody-Unconjugated and HRP-Rabbit Anti-Mouse IgG (H+L) Conjugate were produced by Invitrogen™ (Carlsbad, CA, USA). α-Tubulin (DM1A) Mouse mAb was purchased from Cell Signaling Technology, Inc. (Danvers, MA, USA). Can Get Signal Solution 2 was provided by Toyobo Co., Ltd. (Osaka, Japan). ECL™ western blotting reagents was manufactured by GE Healthcare UK Ltd. (Buckinghamshire, England). BCA Protein Assay Kit was bought from Thermo Fisher Scientific Inc. (Waltham, MA, USA). All other reagents used in the experiments were of analytical grade.

2.1.2 Preparation of CUR suspension in CD formulations

20 mg of CUR were suspended into 1 mL of one of pre-prepared 20-100 mM CD solutions/suspensions in a closed vial. The drug suspension was treated with an ultrasound at 40 kHz at 30 °C for 2 h in a dark room.[57] To test the solubility of CUR in CD solution, the drug suspension was centrifuged at 9660 × *g* for 2 min and then filtered through a 0.45-μm filter. The initial filtrate was discarded and the remaining solution was collected and diluted with 5% (v/v) acetic acid for the assay. The ErS was calculated from the same equation in 1.1.2.

2.1.3 Intestinal absorption of drugs in the presence of CDs

2.1.3.1 Intestinal absorption of CUR in CD formulations

The intestinal absorption was assessed in the same manner as described in 1.1.3. 16.67 mg/mL of CUR was prepared in one of 20-100 mM CD solutions/suspensions in pH 6.5 PBS. Free CUR was dispersed in PBS as the control. All dosing suspensions were treated in the same way as described in 2.1.2. The ErA value was calculated from the same equation in 1.1.3.

2.1.3.2 Intestinal absorption of hydrophilic and poor-absorbable molecules with 50 mM α-CD

In the similar *in situ* closed-loop experiment to the above, CF, FD4, FD10, salmon calcitonin, and insulin were co-administered with 50 mM α-CD solution at the different doses per unit of body weight which were 0.5 mg/kg, 8 mg/kg, 80 μg/kg, and 80 IU/kg, respectively. Free drugs in PBS were used as the controls. The absorptions of salmon calcitonin and insulin were evaluated based on the calcium and glucose concentrations in plasma.

2.1.4 Toxicity study of CDs

2.1.4.1 Intestinal membrane toxicity of CD formulations

In this study, the intestinal membrane toxicity caused by CDs were evaluated based on the quantification of LDH or protein leakage and the morphology of small intestine villi cells.

To measure the LDH activity and the leaked protein from the intestinal tissue, the small intestine was washed with 30 mL of cold PBS (pH 7.4) which was collected from the ileal end and stored in an ice box subsequently. The washing solution was centrifuged at 200 × *g* for 7 min at 4 °C to get rid of any deposition and then was diluted by 100 times for the LDH assay and 10 times for the protein determination. The activity of LDH was determined using the working solution of the cytotoxicity detection kit and the absorbance was read at 490 nm. The

leakage of protein was measured at 595 nm based on the Bradford method.[58] 3% (v/v) TX100 was administered into rat small intestines as a positive control.

The morphology of small intestine villi cells was observed by haematoxylin and eosin (H&E) staining method. To visually identify the damage of the intestinal membrane, the small intestine was examined after the treatment of 50 mM α-CD through an *in situ* closed-loop experiment.[24,59] The small intestinal loop segment was removed and fixed by 4% buffered-formaldehyde. The resulting segment was embedded in a paraffin block, sectioned with thickness at 5 μm, and stained with H&E in order. The stained sections were observed by a light microscopy (BZ-8000 Fluorescence Microscope; KEYENCE Corporation, Osaka, Japan).

2.1.4.2 *In vivo* toxicity of α-CD

In order to obtain the *in vivo* safety evidence, we evaluated the hepatotoxicity of α-CD by testing aspartate transaminase (AST) and alanine transaminase (ALT), and the nephrotoxicity by testing blood urea nitrogen (BUN). Three milliliters of 50 mM α-CD in pH 6.5 PBS was administered intestinally in rats by the *in situ* closed-loop method as described in 1.1.3. PBS was administered as the control. After 240 min treatment, blood samples (~ 0.4 mL) were withdrawn from each group and the plasma was collected immediately by centrifugation at 9660 × *g* for 5 min. The levels of AST and ALT in plasma were measured using the transaminase CII-test Wako, while the assessment of BUN was carried out using Quantichorom™ urea assay kit.

2.1.5 Cellular transport of CF and CUR in the presence of α-CD

2.1.5.1 Cellular transport of CF

Caco-2 cells were cultured as described in 1.1.5.1. All experimental procedures were similar to that in 1.1.5.2, except that 0.5 mL of 10 μM CF in 20 or 50 mM α-CD was added in the apical

compartment. The concentrations of CF were determined by spectrofluorimetry. The same equation in 1.1.5.4 was employed to calculate P_{app} value of each drug. After finishing 6 h of cellular transport study, Caco-2 cellular monolayers were incubated at 37 °C in the cell culture medium and the TEER values were monitored until 24 h.

2.1.5.2 Cellular transport of CUR

Similar to 1.1.5.3, 2 mM CUR in 20 or 50 mM α-CD was prepared as the donor suspension for the cellular transport across Caco-2 cell monolayers. In addition, the concentration of CUR and P_{app} calculation were conducted in the same way as NAT groups.

2.1.6 Western blotting analysis

Western blotting was used to analyze the expression of tight junction-associated proteins in the brush border membrane of rat intestines. The intestine of the male Wister rat was treated with 50 mM α-CD in the same manner as described in the *in situ* closed-loop experiment. The rats were divided into three groups: control, treatment, and recovery group. In the treatment group, the rat small intestine was exposed to the α-CD solution for 90 min and then was removed for the following process. In the recovery group, after 90-min exposure to α-CD, the small intestine was washed with PBS and, 2 h later, was removed in the same method as the treatment group. The PBS-treated small intestine was used as the control. The removed small intestines were excised to extract tight junction-associated proteins in the brush border membrane as per the method in 2.1.7.1. The protein content of each sample was diluted to a final concentration of 5 mg/mL in the homogenizing buffer and the final samples were stored at -80 °C until use.

As one of the tight junction-associated proteins, the expression of claudin-4 was examined in the brush border membrane by a western blotting. Briefly, 20 μL of protein samples were

mixed with SDS buffer solution and separated on a 15% (v/v) polyacrylamide gel at 80 V for 5-6 h by electrophoresis. The separated proteins were electrically transferred to a polyvinylidene difluoride (PVDF) membrane at 15 V for 20 min. The membranes were blocked in 5% (w/v) skim milk in Tris-buffered saline and Tween 20 (TBST) and then incubated with a 1:500 dilution of primary antibodies for claudin-4 and α-tubulin, respectively.[60] Subsequently, after washing three times with TBST, these membranes were incubated with a 1:1000 dilution of HRP-Rabbit Anti-Mouse IgG (H+L) conjugate in *Can get signal solution 2*. After three further washes in TBST, the membranes were exposed to ECL™ western blotting reagents and Chemi-Lumi One Ultra, respectively. The signals were detected by a luminescence imaging system (LAS-4000 mini, FUJIFILM Corporation, Tokyo, Japan). The intensity of the claudin-4 band was corrected by the value obtained from the α-tubulin band as a loading control.

2.1.7 Evaluation of intestinal membrane fluidity in the presence of α-CD

2.1.7.1 Preparation of BBMVs

BBMVs were prepared from the rat intestine by a magnesium precipitation method.[25,26,61] Briefly, after treated as described in the *in situ* closed-loop experiment, the whole small intestine was removed and immersed in the ice-cold PBS (pH 7.4). The intestinal mucosa was collected and homogenized in a homogenizing buffer (pH 7.4), which consisted of 12 mM Tris, 5 mM EGTA, and 300 mM mannitol. The homogenate was added to 10 mM $MgCl_2$, agitated for 15 min at 4 °C, and centrifuged at 3000 × *g* for 10 min at 4 °C. The supernatant was centrifuged at 32000 × *g* for 30 min at 4 °C. The pellets collected from the second centrifugation were suspended in the homogenizing buffer by a 27-gauge needle. The protein concentration was adjusted to 0.1 mg/mL with HEPES-Tris buffer (25 mM HEPES, 5.4 mM KCl, 1.8 mM $CaCl_2$, 0.8 mM $MgSO_4$, 140 mM NaCl, and 5 mM glucose, pH 7.4 modified by 1 M Tris) using a BCA

Protein Assay Kit (Thermo Fisher Scientific Inc., Waltham, MA, USA) with BSA as the standard. This suspension was stored at -80 °C until use.

2.1.7.2 Measurement of intestinal membrane fluidity

To measure the intestinal membrane fluidity, BBMVs were labeled with fluorescent probes by incubating the BBMV suspension with 1 μM DPH, 0.5 μM tma-DPH, or 5 μM DNS-Cl at 37 °C in a dark place and the subsequent addition of 10, 20, and 50 mM α-CD in HEPES-Tris. Cholesterol in BBMV suspension was used as a negative control. The fluorescence intensities of DPH and tma-DPH were detected with an excitation wavelength at 360 nm and emission wavelength at 430 nm, while that of DNS-Cl was measured with an excitation wavelength at 380 nm and emission wavelength at 480 nm, using a fluorescence spectrofluorimeter (F-2000 Spectrofluorimeter; Hitachi Seisakusho Corp, Yokohama, Japan). The fluorescence anisotropy (r) was calculated from the intensity measurements using the following equation:

$$r = (I_{vv} - GI_{vh}) / (I_{vv} + 2GI_{vh})$$

where I_{vv} and I_{vh} represent the fluorescence intensities perpendicular and parallel, respectively to the polarized excitation plane; G represents the compensating factor for the anisotropy sensitivity of the instrument, which was set as 1 in this study.[25,62)]

2.1.8 Statistical analyses

All tests were analyzed in accordance with 1.1.7.

2.2 Results and discussion

2.2.1 Phase solubility study of CUR in CD formulations

As solubilizing agents, various CD solutions were used to improve the solubility of CUR by a sonication method. As indicated in Table 5, 50 mM DM-β-CD showed a highest solubilizing effect to improve the solubility of CUR. The solubility enhancement was related to the concentration of CDs with exception of γ-CD. The enhancing rank order of CD category was DM-β-CD > HP-β-CD > α-CD > β-CD. To understand the interaction between CD and guest molecule, the phase-solubility was studied based on Higuchi and Connors method.[63,64] The phase solubility diagram was plotted using the solubility of CUR versus concentration of CD solution (Fig. 9). The A_L-type phase solubility diagrams were observed with a linear slope ($R > 0.96$). Based on these slopes, the apparent stability constants ($K_{1:1}$) of CUR-CD complexes were calculated as 2980, 4725, 33498, and 116855 M^{-1} for β-, α-, HP-β-, and DM-β-CD, respectively.

In general, the solubilizing effects of the natural CDs on lipophilic compounds are dependent on the size of their inner cavities. Since α-CD showed a superior solubilizing ability, the cavity size of this CD is suitable to the entrapment of CUR molecule. In addition, the surficial modification of β-CD surface by some moieties, such as methyl and hydroxypropyl groups, is capable to raise the solubilizing activity in comparison to the parent. It is possible that chemical modification to the parent CD may facilitate to form H-bond with guest molecules or to form complex aggregates like micelles, resulting in an increase in the extent of drug complexation and interaction.[64,65] As to α-, β-CD, HP-β-CD, and DM-β-CD, they formed the complexes with CUR in a first order stoichiometry of 1:1. These CDs could improve the aqueous solubility of CUR in a concentration-dependent manner.

Table 5 Solubility of CUR in the presence of CD solutions

Group	**Content**	**Solubility (μM)**	**Slope × 10^{-3}**	**Apparent stability constant ($K_{1:1}$) (M^{-1})**	**ErS**
Control	PBS	0.076	--	--	1
α-CD	20 mM	11	0.3590	4725	145
	50 mM	27			355
	100 mM	36			474
β-CD	20 mM	4.7	0.2264	2980	62
	50 mM	11			145
HP-β-CD	20 mM	28	2.5394	33498	368
	50 mM	152			2000
	100 mM	242			3184
DM-β-CD	20 mM	129	8.8028	116855	1697
	50 mM	434			5711
γ-CD	20 mM	0.32	-0.0016	--	4
	50 mM	0.038			0.5
	100 mM	0.022			0.3

(Table 1 in *Int. J. Pharm.* **2018**, *535* (1-2), 340–349)

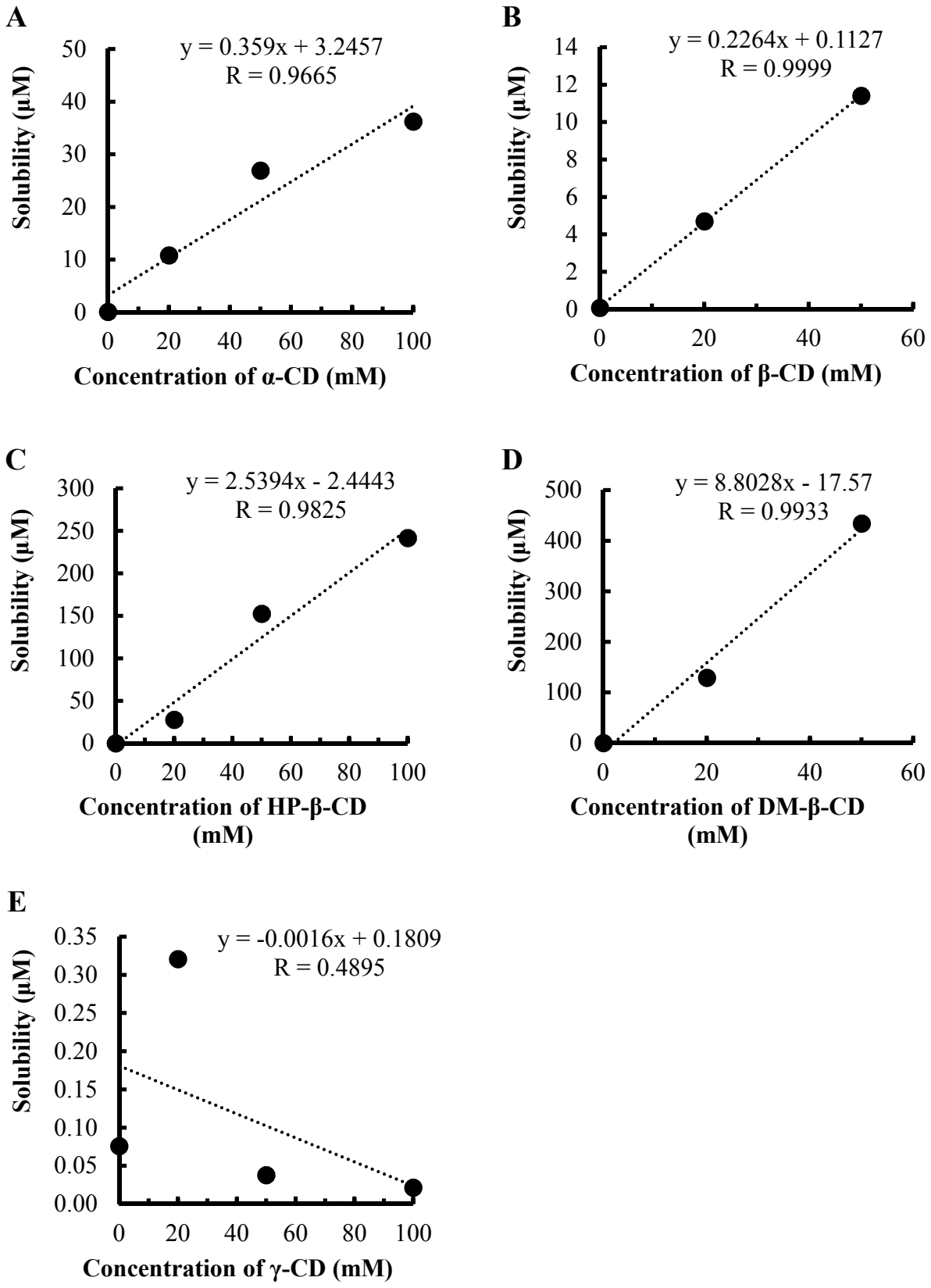

Fig. 9. Phase-solubility diagrams of CUR-CD suspensions

(Reported data in *Int. J. Pharm.* **2018**, *535* (1-2), 340–349)

2.2.2 Intestinal absorption of CUR in the presence of CDs

The intestinal absorption of CUR in CD formulations was studied in the rat small intestine by the *in situ* closed-loop experiment. The plasma concentration of CUR was higher in the presence of 50 or 100 mM α-CD (Fig. 10A) and 20 or 50 mM DM-β-CD (Fig. 10D) than that in the control. In contrast, β-CD (Fig. 10B) and HP-β-CD (Fig. 10C) only exerted a slight increase in the plasma concentration of CUR in rats. γ-CD (Fig. 10E) did not increase the plasma concentrations of CUR, even at the higher concentration. As shown in Table 6, α-CD and DM-β-CD at high concentration increased the intestinal absorption of CUR significantly with an enhancement ratio larger than 2.4. T_{max} of CUR was delayed in the presence of 50 or 100 mM α-CD, and the C_{max} values of CUR were not changed. However, 50 mM DM-β-CD group showed reverse patterns in these parameters.

The absorption enhancement of CUR appeared a concentration dependency to most CDs, except γ-CD. As to α-CD, the delayed T_{max} indicated that there was a time lag of action to improve the absorption in the small intestine. Thus, more care should be taken when α-CD is applied in the oral formulation, because the regular intestinal flow, dilution, and spreading may restrict its absorption-enhancing action. Nevertheless, although the ErA value of DM-β-CD was similar to that of α-CD, the methylated derivative at 50 mM revealed a fast-acting on the absorption based on the shortened T_{max} and increased C_{max} of the polyphenolic compound. To against the fast gastrointestinal transit, this fast action is preferred in the drug development to ameliorate the oral bioavailability of the poorly absorbed drugs. Therefore, α-CD and DM-β-CD may function in different mechanisms to improve the absorption of CUR in rat small intestines.

One possible mechanism of the intestinal absorption of CUR enhanced by CDs is the improved drug solubility in solution. Nevertheless, in terms of the action of HP-β-CD, the intestinal absorption of CUR was not linear with its increased solubility. Furthermore, the

relationship between the solubility and drug absorption in the presence of CDs was investigated by the same method in 1.2.2. The correlation coefficient (R=0.6664; Fig. 11) means that the supersaturated curcumin solution may play a minor role in the drug absorption. Similar to the result in Fig. 3, the rate-limiting step of CUR absorption was shifted from the apparent drug solubility to the permeation in the small intestine when the drug solubility was enhanced more than 5 μg/mL. Therefore, the absorption of CUR in CD formulations could not be completely explained by the enhanced drug solubility in the present study.

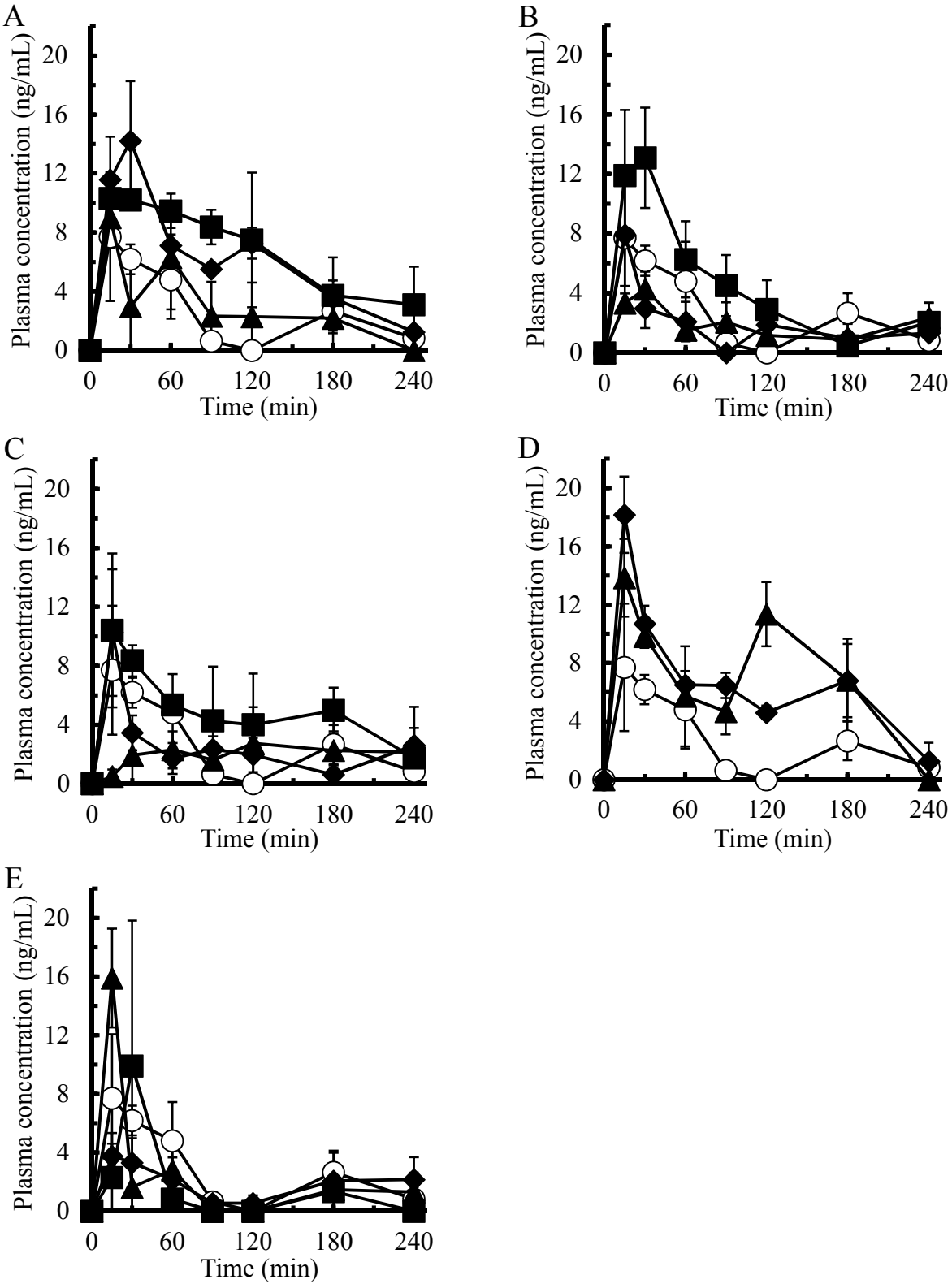

Fig. 10. Absorption of CUR (200 mg/kg) from rat small intestines in the presence of CD solutions (A) α-CD, (B) β-CD, (C) HP-β-CD, (D) DM-β-CD, (E) γ-CD. Keys: (○) CUR (control), (▲) +20 mM, (♦) +50 mM, (■) +100 mM. Results are expressed as the mean ± S.E. of 3-6 experiments. (Fig. 1 in *Int. J. Pharm.* **2018**, *535* (1-2), 340–349)

Table 6 Pharmacokinetic parameters of CUR in the presence of CDs after intestinal administration to rats

Group	**Content**	**C_{max} (ng/mL)**	**T_{max} (min)**	**$AUC_{0–240\ min}$ (ng/mL·min)**	**ErA**
CUR	--	10.75 ± 2.21	30 ± 15	602 ± 62	--
α-CD	20 mM	10.79 ± 1.83	30 ± 15	695 ± 170	1.2
	50 mM	15.11 ± 3.54	60 ± 21	1450 ± 49*	2.4
	100 mM	12.62 ± 0.80	69 ± 22	1574 ± 191**	2.6
β-CD	20 mM	4.37 ± 1.12	49 ± 17	429 ± 51	0.7
	50 mM	10.21 ± 2.59	80 ± 42	431 ± 108	0.7
	100 mM	17.40 ± 3.30	21 ± 4	1016 ± 271	1.7
HP-β-CD	20 mM	5.26 ± 1.56	110 ± 44	492 ± 140	0.8
	50 mM	10.43 ± 4.20	23 ± 4	557 ± 161	0.9
	100 mM	10.92 ± 0.71	19 ± 4	1162 ± 209	1.9
DM-β-CD	20 mM	15.95 ± 2.13	41 ± 26	1661 ± 214**	2.8
	50 mM	18.17 ± 2.62	15 ± 0	1556 ± 179*	2.6
γ-CD	20 mM	4.84 ± 1.47	75 ± 55	425 ± 251	0.7
	50 mM	15.90 ± 3.37	15 ± 0	487 ± 101	0.8
	100 mM	12.10 ± 8.83	90 ± 46	364 ± 210	0.6

Results are expressed as the mean ± S.E. of 3-6 experiments. (**) P< 0.01, (*) P< 0.05, compared with CUR (Control) (Table 2 in *Int. J. Pharm.* **2018**, *535* (1-2), 340–349)

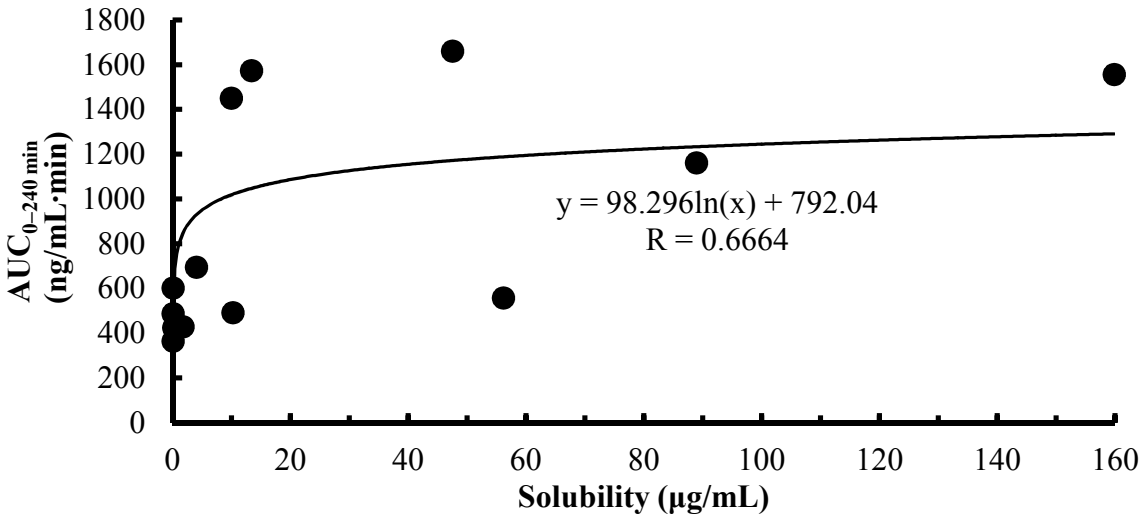

Fig. 11. The relationship between the solubility and intestinal absorption of CUR in the presence of CDs

2.2.3 Intestinal absorption of hydrophilic molecules in 50 mM α-CD solution

To examine the effect of 50 mM α-CD on the intestinal absorption of hydrophilic drugs, CF, FD4, FD10, salmon calcitonin, and insulin were administrated separately into rat small intestines by the *in situ* closed-loop method. As presented in Fig. 12A, B, &C, the absorptions of CF, FD4, and FD10 were higher than that of the control with ErA values at 5.1, 2.6, and 2.3, respectively, upon the co-administration with α-CD. Thus, the absorption-enhancing efficacy of α-CD was limited by the drug molecular weight. In light of the level of the plasma calcium (Fig. 12D), 50 mM α-CD formulation improved the absorption of salmon calcitonin which has a similar molecular weight as FD4. However, the plasma glucose concentration (Fig. 12E) was not changed in the intestinal absorption of insulin with α-CD solution.

By comparing the ErA values between CUR and CF groups, the absorption-enhancing action of α-CD is more effective to the hydrophilic compounds than that to the hydrophobic compounds. This might be explained as that the paracellular pathway is the main route for hydrophilic compound across the intestinal membrane. The dimensions of the paracellular space lie between 10 and 30-50 Å, suggesting that solutes with a molecular radius exceeding

15 Å (~3.5 kDa) will be excluded from this uptake route.[66] Thus, it is plausible that 50 mM α-CD could enhance the paracellular permeation of compounds with a large size up to 10 kDa by opening the tight junctions, based on the absorption enhancements of FD molecules. Furthermore, α-CD enhanced the intestinal absorption of hydrophilic macromolecules with molecular weight near 4000, including the peptide drug, calcitonin. In light of the poor stability of calcitonin in the gastrointestinal tract, it is possible that α-CD would protect calcitonin from proteolysis in the small intestine. On the other hand, α-CD did not exert any effective action to the intestinal delivery of insulin, which might imply that α-CD could not protect the protease cleavage site of insulin.

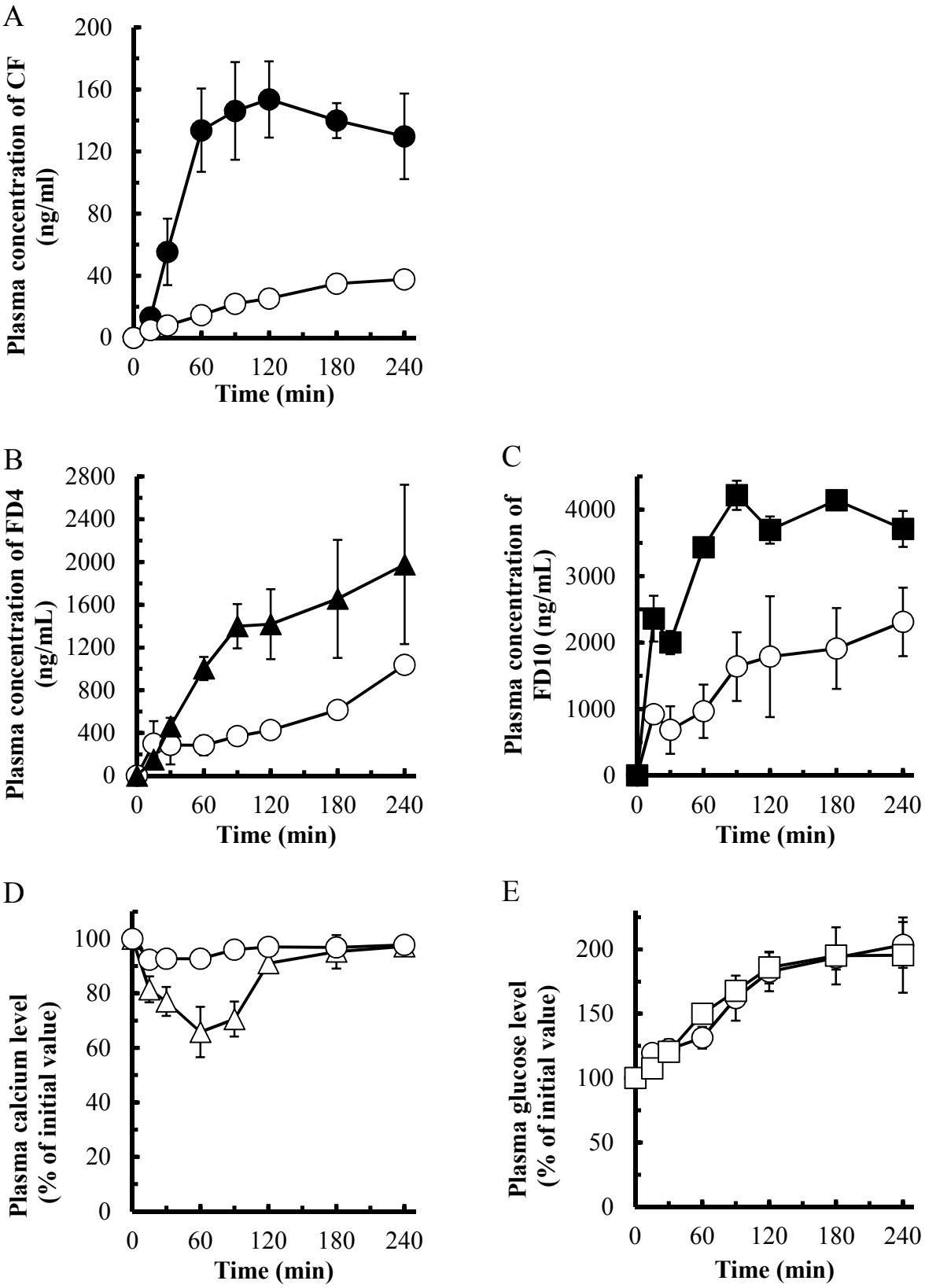

Fig. 12. Effects of 50 mM α-CD on the intestinal absorption of hydrophilic molecules

(A) CF (0.5 mg/kg), (B) FD4, (C) FD10 (8 mg/kg), (D) calcitonin (80 μg/kg), (E) insulin (80 IU/kg).

Open circles are the controls without α-CD. Results are expressed as the mean ± S.E. of 3 experiments.

2.2.4 Toxicity of CDs after intestinal administration

2.2.4.1 Intestinal membrane toxicity of CDs

Both the quantification of biological markers and visualization of the intestinal tissue were used to assess the damage of rat small intestines in the presence of CD solutions. As shown in Fig. 13A, the activity of LDH was significantly increased in 100 mM α-CD, 100 mM β-CD, and 20 or 50 mM DM-β-CD. In addition to the activity of LDH, the level of protein leakage was used to assess the intestinal damage in the administration of CDs (Fig. 13B). 100 mM α-CD, 50 or 100 mM β-CD, 100 mM HP-β-CD, and 50 mM DM-β-CD increased the leakages of proteins from the intestinal mucosa drastically. By contrast, TX100 induced a considerable release of both two markers from the intestinal tissue. The intestinal morphology treated by 50 mM α-CD was displayed in Fig. 14. Compared with the control, there was no any obvious morphological change including denudation of villous tips, desquamation of epithelial surface, and necrosis of the mucosal lamina propria.

The level of proteins in intestinal washing solution is another marker used in the early evaluation of intestinal toxicity when the mucus secretion is stimulated to protect the mucosal damage.[67] The biological markers in Fig. 13 demonstrated that most of the CDs were safe at low concentrations, but might cause intestinal membrane toxicity at high concentration. Compared with other CDs, γ-CD was not toxic in the intestinal administration. These toxic actions might result from the extraction of the lipidic components from the plasma membrane including cholesterol and phospholipids.[68-70] In addition, this toxicity of CDs is related to the modification of their surfaces. For example, the methyl groups may improve the affinity of DM-β-CD to biomembranes, resulting in a large damage to the small intestine.[68] On the other hand, HP-β-CD produced a lower LDH than the parent CD, which might be due to the introduction of hydroxypropyl groups. Overall, based on the high enhancing efficacy and accepted safety,

50 mM α-CD was selected as the optimal absorption enhancer of the tested CD solutions in this study.

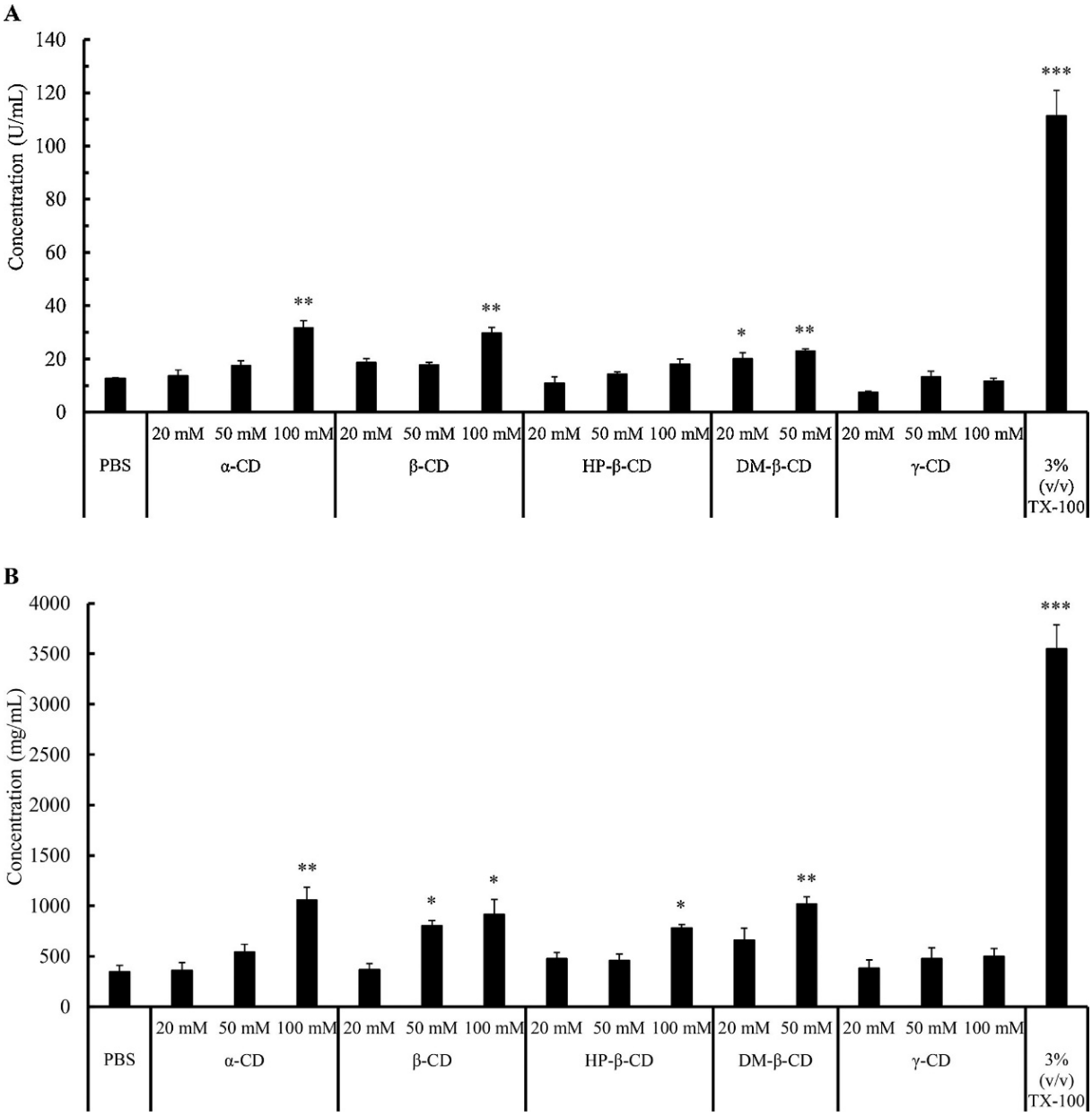

Fig. 13. Measurements of LDH (A) and proteins (B) released from the intestinal membrane in the presence of CDs

Results are expressed as the mean ± S.E. of 3-6 experiments. (***) $p < 0.001$, (**) $p < 0.01$, and (*) $p < 0.05$, compared with the control. (Fig. 2 in *Int. J. Pharm.* **2018**, *535* (1-2), 340–349)

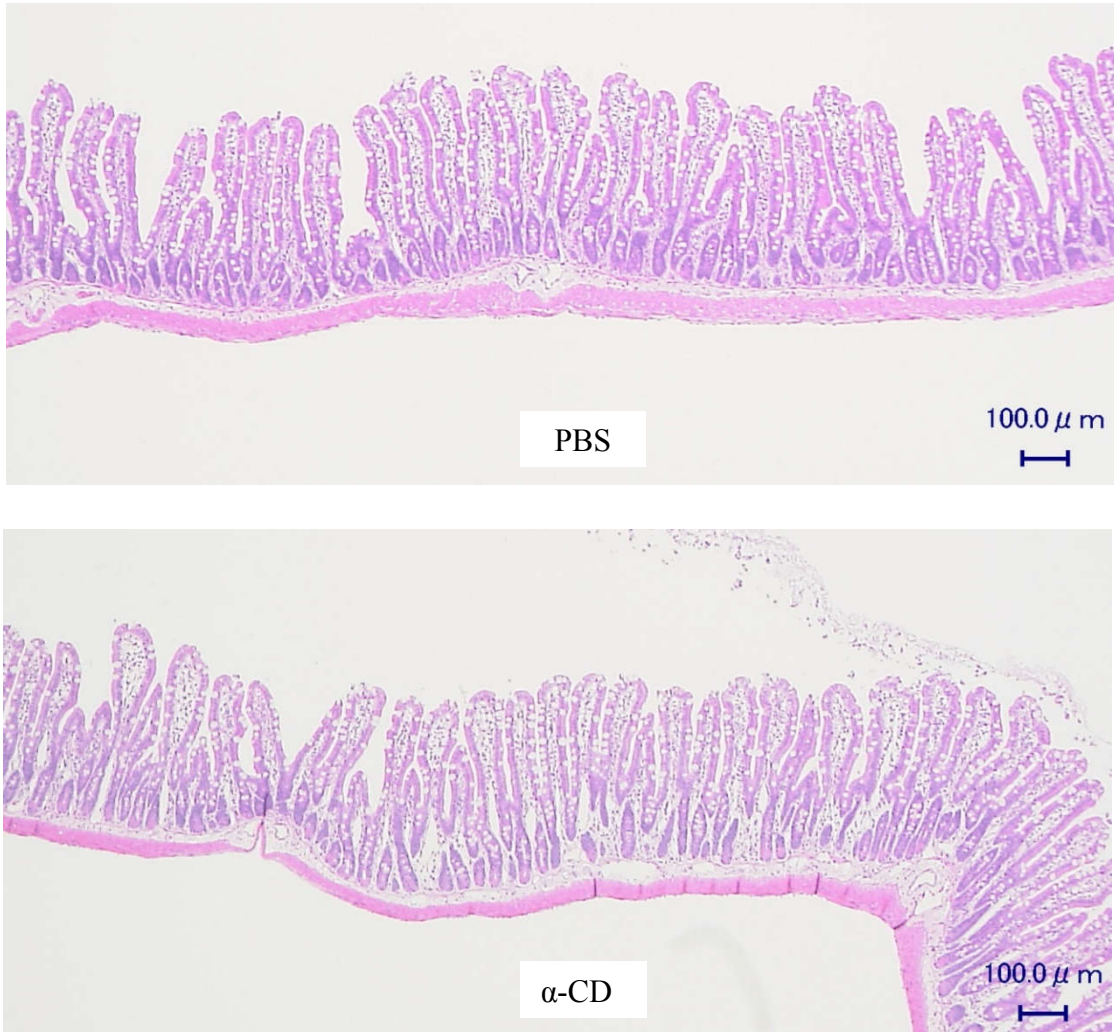

Fig. 14. Histological micrographs of rat small intestinal tissue treated with 50 mM α-CD

2.2.4.2 Systemic toxicity of 50 mM α-CD after intestinal administration

To obtain the *in vivo* safety evidence, hepatotoxicity and nephrotoxicity of α-CD after intestinal administration were evaluated by measuring the levels of plasma AST, ALT, and BUN. The results in Fig. 15 show that all toxicity indexes displayed similar results between 50 mM α-CD treatment group and the control. Thus, α-CD may not impair both liver and kidney functions in the intestinal administration.

It is regarded that the toxicity of CDs in oral administration is low because their basic component of glucose. Generally, most of the CDs are too large to be absorbed and then are digested by bacteria in the gastrointestinal tract. In addition, oral administration of α-CD is well

tolerated, and as a dietary supplement, the total daily oral dose of α-CD can reach 6000 mg/day.[71] When 50 mM α-CD in 3 mL was used in the present absorption experiment, the amount of α-CD was equal to 5674 mg for a human with a body weight of 60 kg.[72] Therefore, it is eligible to use 50 mM α-CD as an oral delivery vehicle in the formulation.

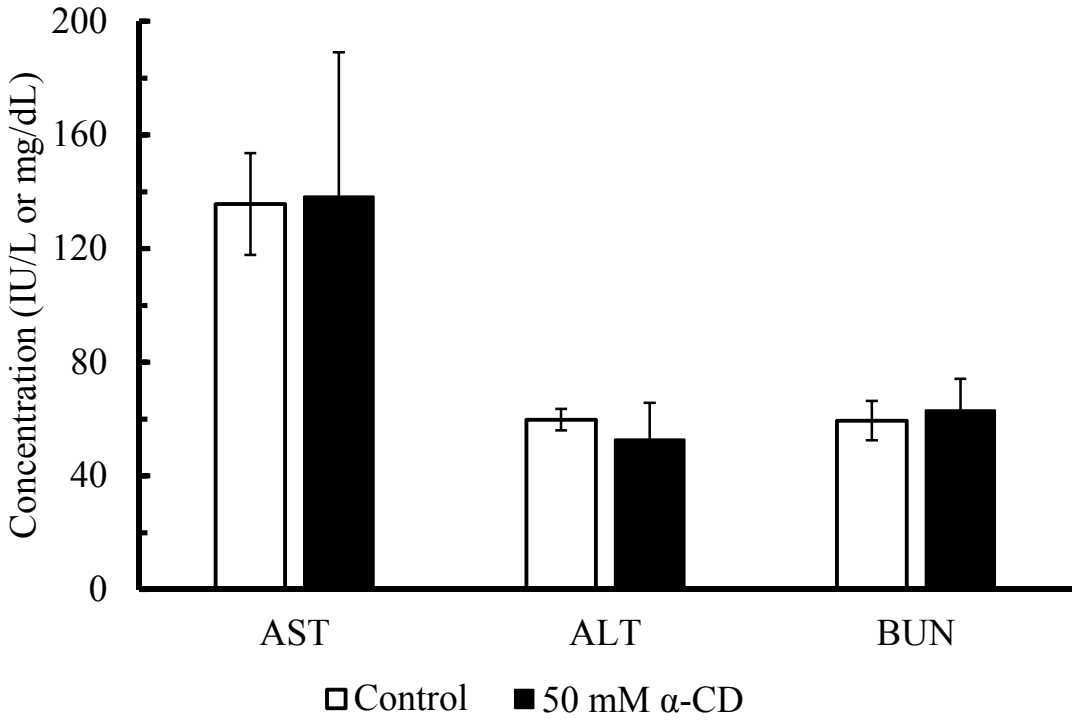

Fig. 15. Hepatotoxicity and nephrotoxicity of 50 mM α-CD after intestinal administration
The empty bar is the control; the black bar is treated by α-CD. Results are expressed as the mean ± S.E. of 2-3 experiments.

2.2.5 Effects of α-CD on the permeation of poorly absorbable compounds across Caco-2 cell monolayers.

Caco-2 cell models were used to elucidate the influence of α-CD on the paracellular permeation of poorly absorbable compounds. The TEER value in Fig. 16A showed a gradual decrease in the presence of 50 mM α-CD, which reached 51% of the initial value after a 90-min incubation. In contrast, in 20 mM α-CD, TEER appeared a similar trend as that of the control in a majority of the time. Consequently, the cellular transport of drugs was significantly

increased by the addition of 50 mM α-CD (Fig. 16B&C). The P_{app} values of CF and CUR rose to $(8.39 \pm 0.40) \times 10^{-6}$ and $(0.91 \pm 0.02) \times 10^{-6}$, respectively.

High concentration of α-CD can alter the barrier function of Caco-2 cells and improve the drug permeation via the paracellular pathway. This alteration was temporary and reversible in view of the fact that the decreased TEER value recovered and returned to the initial level after removing 50 mM α-CD. In terms of P_{app} values, the permeability of CF was 65-fold higher in 50 mM α-CD than that in the control, while the value of CUR was increased to 130% by the same α-CD solution. These results suggest that the enhanced paracellular permeation may contribute to the intestinal absorption of these compounds.

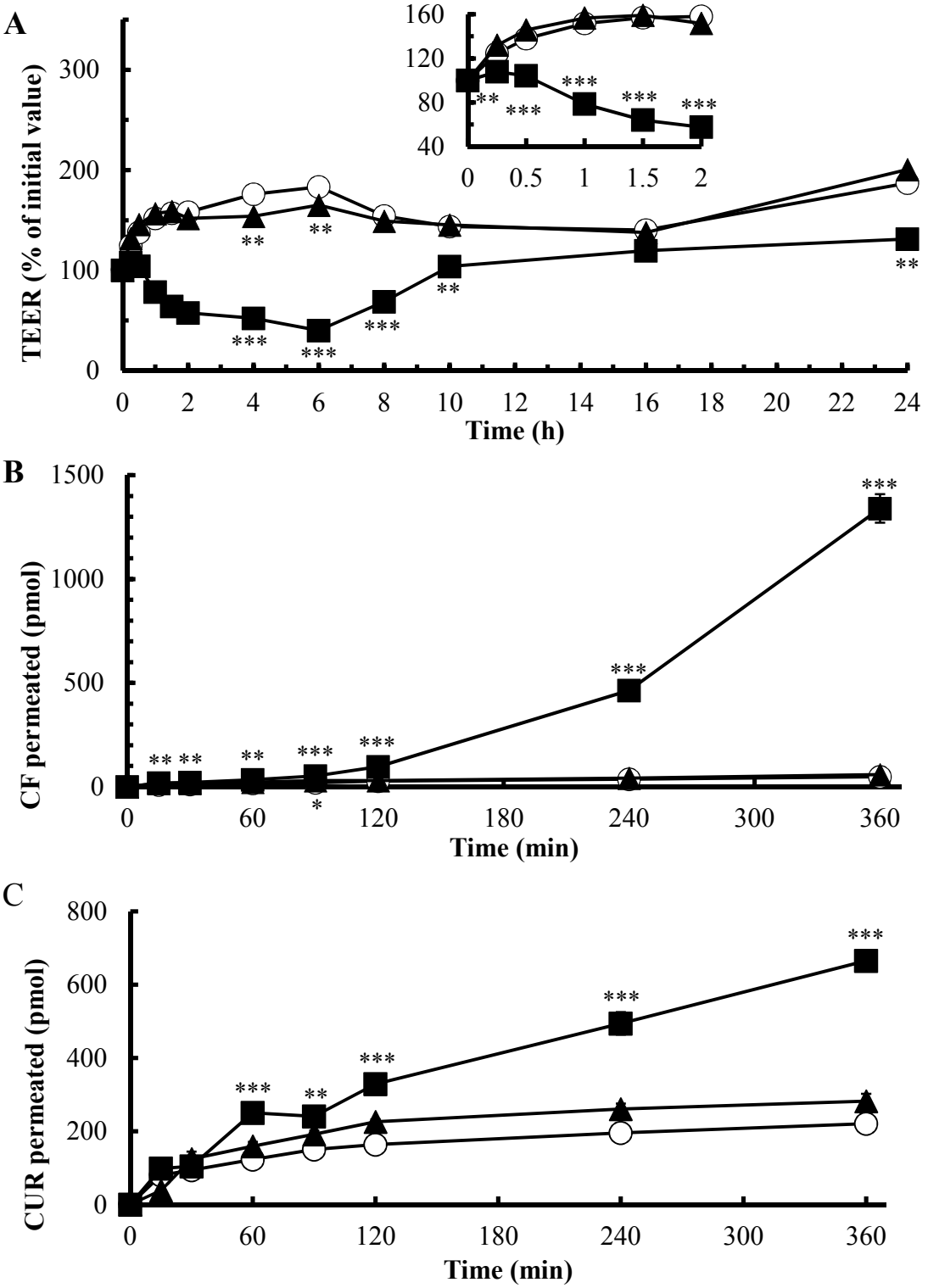

Fig. 16. Cellular transport of CF and CUR in the presence of α-CD

(A) TEER, (B) the permeated amount of CF (B) and CUR (C). Keys: (○) Control, (▲) +20 mM α-CD, (■) +50 mM α-CD. (***) $p < 0.001$, (**) $p < 0.01$, and (*) $p < 0.05$, compared with the control. Results are expressed as the mean ± S.E. of 3 experiments. Some S.E. error bars are within the size of symbols. (Fig. 3 in *Int. J. Pharm.* **2018**, *535* (1-2), 340–349)

2.2.6 Expression of claudin-4 in the presence of 50 mM α-CD

The expression of the tight junction-associated protein, claudin-4, was measured by a western blotting analysis. After the rat small intestine was treated with 50 mM α-CD solution, the level of the typical protein expressed in the intestinal membrane was shown in Fig. 17. The luminescence intensity of claudin-4 in the treatment group was approximately 60% of that in the control (Fig. 17A&B). On the other hand, the amount of the same protein in the recovery group was about 80% of the control, after washing α-CD solution (Fig. 17C&D).

The expression of the claudin-family tight junction proteins is critical for the formation of tight junction strands that regulate the diffusion of many solutes through the paracellular pathway.[60] Based on the distribution of claudins, claudin-4 was examined as a key protein expressed in the intestinal tissue. The deduction of the protein expression (Fig. 17A&B) means the disruption of tight junctions in the paracellular pathway, which is consistent with the enhanced paracellular permeation on Caco-2 cell monolayers. Furthermore, the reassembly of claudin-4 (Fig. 17C&D) was observed after removing the CD solution, suggesting the re-formation of tight-junction strands. Therefore, it is possible that 50 mM α-CD may open the tight junctions reversibly in the paracellular pathway and promote the intestinal absorption of CUR temporarily.

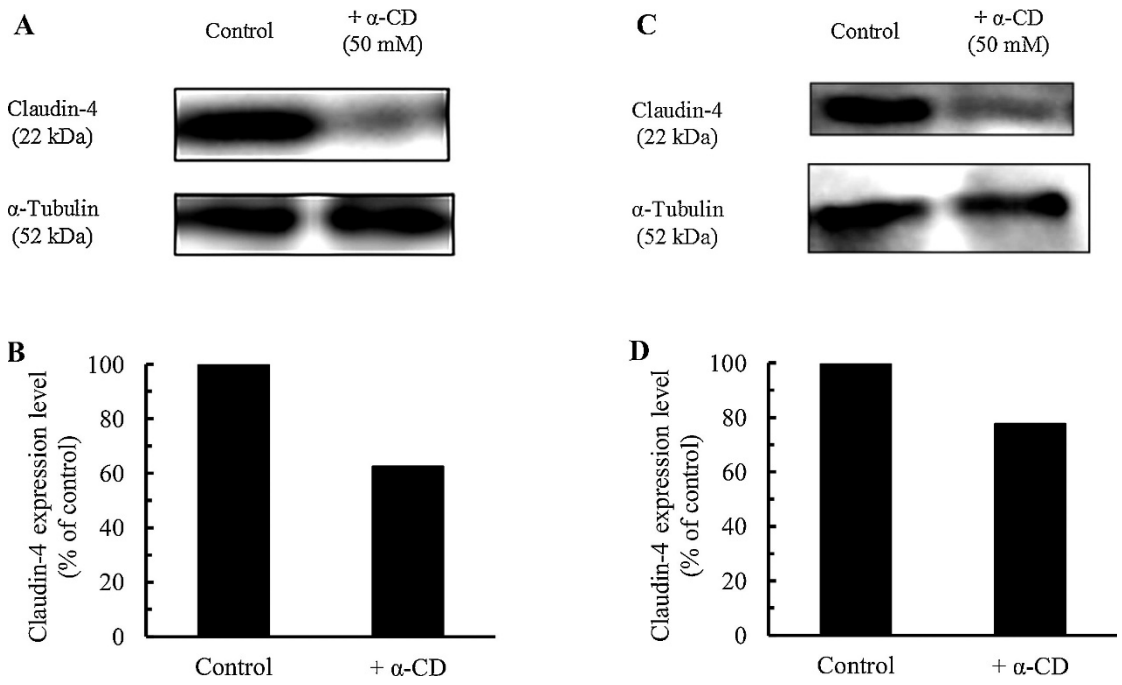

Fig. 17. Reduction and recovery of claudin-4 expression after the treatment with 50 mM α-CD (A) Western blotting analysis of claudin-4 in the treatment group, (B) the density of claudin-4 in the treatment group, (C) western blotting analysis of claudin-4 in the recovery group, (D) the density of claudin-4 in the recovery group. (Fig. 4 in *Int. J. Pharm.* **2018**, *535* (1-2), 340–349)

2.2.7 Effects of α-CD on the membrane fluidity

The effects of different concentrations of α-CD on the membrane fluidity were evaluated by examining the fluorescence anisotropy of various fluorescent probes labeled in lipid bilayers of enterocytes. As depicted in Fig. 18A, the fluorescence anisotropy of DPH, a marker probe for the inner lipid layer, declined significantly in the presence of 10-50 mM α-CD solutions. As a marker probe for the surface of lipid bilayers, a remarkable decrease in the fluorescence anisotropy of tma-DPH was detected only in the presence of 50 mM α-CD (Fig. 18B). In contrast, regarding the protein region, α-CD exhibited a bi-directional effect on the fluorescence

anisotropy of DNS-Cl. That is, the fluorescence anisotropy of DNS-Cl was decreased by α-CD at 10 mM, but increased at 50 mM (Fig. 18C).

DPH and tma-DPH represent the inner and surface regions of lipid bilayers of the membrane, respectively. The decreased fluorescence anisotropies of DPH and tma-DPH were dependent on the concentration of α-CD solution. In addition, in the comparison of the results between Fig. 18A and B, α-CD displayed a more intense effect on the inner part than the outside of phospholipids. Contrarily, the variation of the fluorescence anisotropy of DNS-Cl suggests a complex interaction between α-CD and the protein of biomembranes. When the membrane fluidity increases, the fluorescent molecules tumble quickly and have depolarized emission, thus displaying low fluorescence anisotropy.[73] Therefore, these results indicated that α-CD increased the membrane fluidity of lipid bilayers, which may subsequently improve the intestinal absorption of CUR via a transcellular pathway.

However, the precise mechanisms of the actions of α-CD on the barrier function of the intestinal membrane were not fully understood in the present study. Since we observed a concentration-dependent increase in LDH release and anisotropy data, the increased membrane fluidity may be ascribed to the extraction of lipid components by α-CD. Moreover, α-CD increased the cellular transport of CF in a concentration-dependent manner. Thus, these actions might be related to the extraction of lipid components of the intestinal membrane. Generally, absorption enhancers could increase the membrane fluidity by disrupting the membrane stiffness, and open the tight junction by changing the tight junction protein related Ca^{2+} level or by modifying the structural components of the cytoskeleton.[74] Therefore, it is assumed that the lipid-extracting ability of α-CD would play an important role in the permeation via paracellular and transcellular pathways.

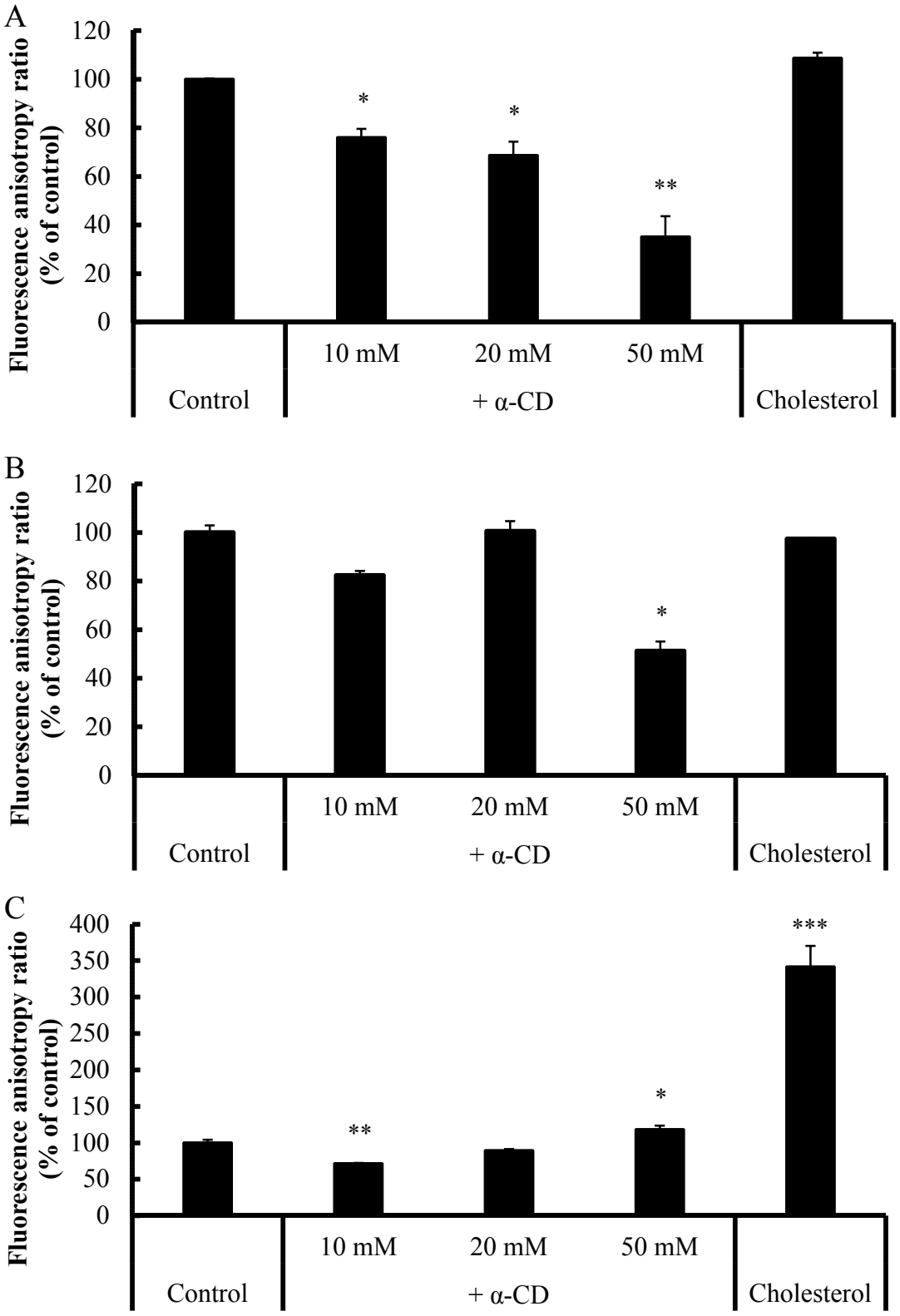

Fig. 18. Fluorescence anisotropy of DPH (A), tma-DPH (B), and DNS-Cl (C) in the presence of α-CD

Results are expressed as the mean ± S.E. of 3 experiments. (***) $p < 0.001$, (**) $p < 0.01$, and (*) $p < 0.05$, compared with the control. (Fig. 5 in *Int. J. Pharm.* **2018**, *535* (1-2), 340–349)

2.3 Conclusions

In this chapter, the solubility and intestinal absorption of CUR were studied by co-administration with various CDs at different concentrations. Particularly, 50mM α-CD is the optimal vehicle of the tested CD formulations, which significantly enhanced not only the poorly aqueous solubility of CUR but also its absorption in rat small intestine with an evident safety. In addition, 50 mM α-CD increased the low intestinal absorption of hydrophilic molecules including CF, FD4, FD10, and salmon calcitonin. The cellular transport study and western blotting analysis demonstrated that 50 mM α-CD had a strong action to promote the paracellular permeation of poorly absorbed drug by opening the tight junction through the regulation of the expression of claudin-4. Furthermore, the intestinal membrane fluidity study indicated that α-CD may have promoted the drug permeation via the transcellular pathway by increasing the intestinal membrane fluidity. Therefore, it is concluded that 50 mM α-CD is able to alter the barrier properties of both paracellular and transcellular pathways, resulting in an enhanced intestinal absorption of CUR.

Summary

As shown in Fig. 3 and Fig. 11, when the solubility was higher than 5 μg/mL, the rate-limiting step of CUR absorption was shifted from the apparent drug solubility to the permeation across the intestinal membrane, which confirmed the drawbacks of CUR in both solubility and permeability. Therefore, the intestinal absorption enhancements induced by absorption enhancers might be attributed to the synergistic effect of enhanced solubility and permeability of CUR in their presence. The detailed summaries of specific chapters are listed as below.

Chapter I

1) In the presence of 1% (v/v) of either CMT or LMT, the solubility of CUR was more than 4000-fold higher than that in the control. The rank order of the solubilizing effect was CMT > LMT > MMT > SMT > PMT.

2) The intestinal absorption of CUR was enhanced significantly by 1% (v/v) of either CMT or LMT with an enhancement ratio at 42~47, compared with the native compound. The rank order of the absorption-enhancing ability was LMT ≥ MMT ≥ CMT > SMT > PMT.

3) None of the tested NATs induced any intestinal membrane damage in terms of the LDH activity.

4) Both CMT and LMT decreased the cellular TEER value in a concentration-dependent manner when Caco-2 cells were exposed to 0.003-0.1% (v/v) of either CMT or LMT. These

findings suggest that the absorption-enhancing mechanism of both two taurates may be partly linked to the opening of the tight junction in the paracellular pathway.

5) The P_{app} values of CF across cellular layers were improved from $(0.13 \pm 0.01) \times 10^{-6}$ cm/s in the control to $(12.58 \pm 0.73) \times 10^{-6}$ and $(11.61 \pm 0.21) \times 10^{-6}$ cm/s in 0.1% CMT and LMT solution, respectively. Similarly, the permeability of CUR was increased from $(0.70 \pm 0.04) \times 10^{-6}$ cm/s in free CUR suspension to $(5.36 \pm 0.60) \times 10^{-6}$ and $(6.74 \pm 0.38) \times 10^{-6}$ cm/s in CMT and LMT solutions, respectively.

Chapter II

1) 4 types of CDs, except for γ-CD, increased the solubility of CUR from nanogram level to microgram level in aqueous solution. The solubilizing ability of CDs was DM-β-CD > HP-β-CD > α-CD > β-CD. The interaction between CUR and CD molecule was investigated by phase-solubility diagrams, suggesting that 1:1 complex was formed in the solution.

2) In the intestinal absorption of CUR, 50 mM α-CD was regarded as the optimal absorption enhancers of the tested CD formulation based on its high enhancing efficacy and accepted safety to the intestinal tissue, liver, and kidney.

3) 50 mM α-CD increased the intestinal absorption of hydrophilic molecules including CF, FD4, FD10, and salmon calcitonin.

4) α-CD at 50 mM rather than 20 mM decreased the TEER values of Caco-2 cells reversibly, resulting in a temporary permeation through the paracellular pathway. With the addition of

50 mM α-CD, the P_{app} values of CF and CUR increased to $(8.39 \pm 0.40) \times 10^{-6}$ and $(0.91 \pm 0.02) \times 10^{-6}$, respectively.

5) The enhanced paracellular permeation by 50 mM α-CD was ascribed to the disruption of the tight junction based on the expression of intestinal claudin-4, a tight-junction associated protein, in western blotting analysis.

6) In the membrane fluidity study, the decreased fluorescence anisotropies of DPH and tma-DPH suggested that the accelerated membrane fluidity of lipid bilayers induced by 10-50 mM α-CD may promote the intestinal absorption of CUR via a transcellular pathway.

Acknowledgement

I am greatly indebted to all of my family members for their support and understanding. Especially, I would like to express my deepest appreciation to my wife, Ms. Xinying Hu, for replacing me to shoulder the burden of raising babies.

I wish to express my sincere gratitude to my supervisor, Dr. Akira Yamamoto for providing me this precious opportunity as a Ph.D. student in his laboratory. Discussion with him about the absorption enhancers and their mechanisms gave me the capacity to improve the drug absorption of poorly absorbed molecules. I also appreciate Dr. Changqing Yang and Dr. Kenichi Inui for their guidance in my academic study.

I always greatly appreciate the comments and suggestions offered by Dr. Toshiyasu Sakane, Dr. Hidemasa Katsumi, Dr. Kosuke Kusamori, and Dr. Masaki Morishita. Their inspiring thought and hospitality during my study were unforgettable.

I would like to give my special thanks to Dr. Hiroyuki Yasui and Dr. Hiroyuki Saito for the detailed evaluation and invaluable comments on my Ph.D. dissertation.

I would like to thank Mr. Shunsuke Kimura for HPLC method of curcumin assay, thank Dr. Wanting zhao, Dr. Yuka Nakaya, and Ms. Akiko Tanaka for the operations in animal study, thank Mr. Kasirawat Sawangrat for the culture method of Caco-2 cells, thank Ms. Sachiyo Uehara for the western blotting and membrane fluidity tests, thank Ms. Ami Kawamura and Mr. Yusuke Sato for the experiments using *N*-acyl taurates, and thank Ms. Ann Omokawa and Ms. Hatsumi Yamaguchi for LDH and protein values of the positive control.

This study was supported in part by Kyoto Pharmaceutical University Scholarship for International Students, Zhang Fen Jun Scholarship Fund (Kyoto City International Foundation), and JASSO (Japan Student Services Organization).

Finally, I am grateful to everyone in my life. Many thanks for your insightful comments and generous help.

References

1) Araújo, C.C.; Leon, L.L. Biological activities of Curcuma longa L. *Mem. Inst. Oswaldo Cruz* **2001**, *96* (5), 723–728.

2) Aggarwal, B.B.; Harikumar, K.B. Potential therapeutic effects of curcumin, the anti-inflammatory agent, against neurodegenerative, cardiovascular, pulmonary, metabolic, autoimmune and neoplastic diseases. *Int. J. Biochem. Cell Biol.* **2009**, *41* (1), 40–59.

3) Goel, A; Kunnumakkara, A.B.; Aggarwal, B.B. Curcumin as "Curecumin": from kitchen to clinic. *Biochem. Pharmacol.* **2008**, *75* (4), 787–809.

4) Srivastava, R.M.; Singh, S.; Dubey, S.K.; Misra, K.; Khar, A. Immunomodulatory and therapeutic activity of curcumin. *Int. Immunopharmacol.* **2011**, *11* (3), 331–341.

5) Kurita, T.; Makino, Y. Novel curcumin oral delivery systems. *Anticancer Res.* **2013**, *33* (7), 2807–2821.

6) Naksuriya, O.; Okonogi, S.; Schiffelers, R.M.; Hennink, W.E. Curcumin nanoformulations: a review of pharmaceutical properties and preclinical studies and clinical data related to cancer treatment. *Biomaterials* **2014**, *35* (10), 3365–3383.

7) Antiga, E.; Bonciolini, V.; Volpi, W.; Bianco, E.D.; Caproni, M. Oral curcumin (Meriva) is effective as an adjuvant treatment and is able to reduce IL-22 serum levels in patients with psoriasis vulgaris. *Biomed Res. Int.* **2015**, *2015*, 283634.

8) Lao, C.D.; Ruffin, M.T. 4th; Normolle. D.; Heath, D.D.; Murray, S.I.; Bailey, J.M.; Boggs, M.E.; Crowell, J.; Rock, C.L.; Brenner, D.E. Dose escalation of a curcuminoid formulation. *BMC Complement. Altern. Med.* **2006**, *6*, 10.

9) Anand, P.; Kunnumakkara, A.B.; Newman, R.A.; Aggarwal, B.B. Bioavailability of curcumin: problems and promises. *Mol. Pharm.* **2007**, *4* (6), 807–818.

10) Mehanny, M.; Hathout, R.M.; Geneidi, A.S.; Mansour, S. Exploring the use of nanocarrier systems to deliver the magical molecule; Curcumin and its derivatives. *J. Control. Release* **2016**, *225*, 1–30.

11) Shoba, G.; Joy, D.; Joseph, T.; Majeed, M.; Rajendran, R.; Srinivas, P.S. Influence of piperine on the pharmacokinetics of curcumin in animals and human volunteers. *Planta Med.* **1998**, *64* (4), 353–356.

12) Wichitnithad, W.; Nimmannit, U.; Wacharasindhu, S.; Rojsitthisak P. Synthesis, characterization and biological evaluation of succinate prodrugs of curcuminoids for colon cancer treatment. *Molecules* **2011**, *16* (2), 1888–1900.

13) Kimura, S.; Kasatani, S.; Tanaka, M.; Araki, K.; Enomura, M.; Moriyama, K.; Inoue, D.; Furubayashi, T.; Tanaka, A.; Kusamori, K.; Katsumi, H.; Sakane, T.; Yamamoto, A. Importance of the direct contact of amorphous solid particles with the surface of monolayers for the transepithelial permeation of curcumin. *Mol. Pharm.* **2016**, *13* (2), 493–499.

14) Maher, S.; Mrsny, R.J.; Brayden, D.J. Intestinal permeation enhancers for oral peptide delivery. *Adv. Drug Deliv. Rev.* **2016**, *106* (Pt B), 277–319.

15) Aguirre, T.A.; Teijeiro-Osorio, D.; Rosa, M.; Coulter, I.S.; Alonso, M.J.; Brayden, D.J. Current status of selected oral peptide technologies in advanced preclinical development and in clinical trials. *Adv. Drug Deliv. Rev.* **2016**, *106* (Pt B), 223–241.

16) Murakami, M.; Kusanoi, Y.; Takada, K.; Muranishi, S. Assessment of enhancing ability of medium-chain alkyl saccharides as new absorption enhancers in rat rectum. *Int. J. Pharm.* **1992**, *79* (1-3), 159–169.

17) Uchiyama, T.; Yamamoto, A.; Hatano, H.; Fujita, T.; Muranishi, S. Effectiveness and toxicity screening of various absorption enhancers in the large intestine: intestinal absorption of phenol red and protein and phospholipid release from the intestinal membrane. *Biol. Pharm. Bull.* **1996**, *19* (12), 1618–1621.

18) Yamamoto, A.; Uchiyama, T.; Nishikawa, R.; Fujita, T.; Muranishi, S. Effectiveness and toxicity screening of various absorption enhancers in the rat small intestine: effects of absorption enhancers on the intestinal absorption of phenol red and the release of protein and phospholipids from the intestinal membrane. *J. Pharm. Pharmacol.* **1996**, *48* (12), 1285–1289.

19) Fujita, T.; Fujita, T.; Morikawa, K.; Tanaka, H.; Iemura, O.; Yamamoto, A.; Muranishi S. Improvement of intestinal absorption of human calcitonin by chemical modification with fatty acids: synergistic effects of acylation and absorption enhancers. *Int. J. Pharm.* **1996**, *134* (1-2), 47–57.

20) Yamamoto, A.; Okagawa, T.; Kotani, A.; Uchiyama, T.; Shimura, T.; Tabata, S.; Kondo, S.; Muranishi, S. Effects of different absorption enhancers on the permeation of ebiratide, an ACTH analogue, across intestinal membranes. *J. Pharm. Pharmacol.* **1997**, *49* (11), 1057–1061.

21) Uchiyama, T.; Kotani, A.; Kishida, T.; Tatsumi, H.; Okamoto, A.; Fujita, T.; Murakami, M.; Muranishi, S.; Yamamoto, A. Effects of various protease inhibitors on the stability and permeability of [D-Ala^2,D-Leu^5]enkephalin in the rat intestine: comparison with leucine enkephalin. *J. Pharm. Sci.* **1998**, *87* (4), 448–452.

22) Uchiyama, T.; Sugiyama, T.; Quan, Y.S.; Kotani, A.; Okada, N.; Fujita, T.; Muranishi, S.; Yamamoto, A. Enhanced permeability of insulin across the rat intestinal membrane by various absorption enhancers: their intestinal mucosal toxicity and absorption-enhancing mechanism of n-lauryl-beta-D-maltopyranoside. *J. Pharm. Pharmacol.* **1999**, *51* (11), 1241–1250.

23) Quan, Y.S.; Fujita, T.; Tohara, D.; Tsuji, M.; Kohyama, M.; Yamamoto, A. Transport kinetics of leucine enkephalin across Caco-2 monolayers: quantitative analysis for contribution of enzymatic and transport barrier. *Life Sci.* **1999**, *64* (14), 1243–1252.

24) Alama, T.; Kusamori, K.; Katsumi, H.; Sakane, T.; Yamamoto, A. Absorption-enhancing effects of gemini surfactant on the intestinal absorption of poorly absorbed hydrophilic drugs including peptide and protein drugs in rats. *Int. J. Pharm.* **2016**, *499* (1-2), 58–66.

25) Alama, T.; Katayama, H.; Hirai, S.; Ono, S.; Kajiyama, A.; Kusamori, K.; Katsumi, H.; Sakane, T.; Yamamoto, A. Enhanced oral delivery of alendronate by sucrose fatty acids esters in rats and their absorption-enhancing mechanisms. *Int. J. Pharm.* **2016**, *515* (1-2), 476–489.

26) Nakaya, Y.; Takaya, M.; Hinatsu, Y.; Alama, T.; Kusamori, K.; Katsumi, H.; Sakane, T.; Yamamoto, A. Enhanced oral delivery of bisphosphonate by novel absorption enhancers: improvement of intestinal absorption of alendronate by *N*-acyl amino acids and *N*-acyl taurates and their absorption-enhancing mechanisms. *J. Pharm. Sci.* **2016**, *105* (12), 3680–3690.

27) Yamamoto, A.; Muranishi, S. Rectal drug delivery systems Improvement of rectal peptide absorption by absorption enhancers, protease inhibitors and chemical modification. *Adv. Drug Deliv. Rev.* **1997**, *28* (2), 275–299.

28) Fujita, T.; Kawahara, I.; Quan, Y.; Hattori, K.; Takenaka, K.; Muranishi, S.; Yamamoto, A. Permeability characteristics of tetragastrins across intestinal membranes using the Caco-2 monolayer system: comparison between acylation and application of protease inhibitors. *Pharm. Res.* **1998**, *15* (9), 1387–1392.

29) Tozaki, H.; Odoriba, T.; Iseki, T.; Taniguchi, T.; Fujita, T.; Murakami, M.; Muranishi, S.; Yamamoto, A. Use of protease inhibitors to improve calcitonin absorption from the small and large intestine in rats. *J. Pharm. Pharmacol.* **1998**, *50* (8), 913–920.

30) Fetih, G.; Habib, F.; Katsumi, H.; Okada, N.; Fujita, T.; Attia, M.; Yamamoto, A. Excellent absorption enhancing characteristics of NO donors for improving the intestinal absorption

of poorly absorbable compound compared with conventional absorption enhancers. *Drug Metab. Pharmacokinet.* **2006**, *21* (3), 222–229.

31) Dong, Z.; Katsumi, H.; Sakane, T.; Yamamoto, A. Effects of polyamidoamine (PAMAM) dendrimers on the nasal absorption of poorly absorbable drugs in rats. *Int. J. Pharm.* **2010**, *393* (1-2), 244–252.

32) Dong, Z.; Hamid, K.A.; Gao, Y.; Lin, Y.; Katsumi, H.; Sakane, T.; Yamamoto, A. Polyamidoamine dendrimers can improve the pulmonary absorption of insulin and calcitonin in rats. *J. Pharm. Sci.* **2011**, *100* (5), 1866–1878.

33) Shen, Q.; Li, W.; Lin, Y.; Katsumi, H.; Okada, N.; Sakane, T.; Fujita, T.; Yamamoto, A. Modulating effect of polyethylene glycol on the intestinal transport and absorption of prednisolone, methylprednisolone and quinidine in rats by in-vitro and in-situ absorption studies. *J. Pharm. Pharmacol.* **2008**, *60* (12), 1633–1641.

34) Zhao, W.; Uehera, S.; Tanaka, K.; Tadokoro, S.; Kusamori, K.; Katsumi, H.; Sakane, T.; Yamamoto, A. Effects of Polyoxyethylene Alkyl Ethers on the Intestinal transport and absorption of Rhodamine 123: A P-glycoprotein substrate by in vitro and *in vivo* studies. *J. Pharm. Sci.* **2016**, *105* (4), 1526–1534.

35) Esatbeyoglu, T.; Huebbe, P.; Ernst, I.M.; Chin, D.; Wagner, A.E.; Rimbach, G. Curcumin--from molecule to biological function. *Angew. Chem. Int. Ed. Engl.* **2012**, *51* (22), 5308–5332.

36) Tønnesen, H.H.; Másson, M.; Loftsson, T. Studies of curcumin and curcuminoids. XXVII. Cyclodextrin complexation: solubility, chemical and photochemical stability. *Int. J. Pharm.* **2002**, *244* (1-2), 127–135.

37) Tønnesen, H.H.; Karlsen, J. Studies on curcumin and curcuminoids. VI. Kinetics of curcumin degradation in aqueous solution. *Z. Lebensm. Unters. Forsch.* **1985**, *180* (5), 402–404.

38) Morán, M.C.; Pinazo, A.; Pérez, L.; Clapés, P.; Angelet, M.; García, M.T.; Vinardell, M.P.; Infante, M.R. "Green" amino acid-based surfactants. *Green Chem.* **2004**, *6*, 233–240.

39) Petter, P.J. Fatty acid sulphoalkyl amides and esters as cosmetic surfactants. *Int. J. Cosmet. Sci.* **1984**, *6* (5), 249–260.

40) Hibbs, J. Anionic surfactants. In *Chemistry and Technology of Surfactants*; Farn, R. J., Eds.; Blackwell Publishing: Oxford, UK, **2006**; pp 130–132.

41) Saghatelian, A.; McKinney, M.K.; Bandell, M.; Patapoutian, A.; Cravatt, B.F. A FAAH-regulated class of *N*-acyl taurines that activates TRP ion channels. *Biochemistry* **2006**, *45* (30), 9007–9015.

42) Sasso, O.; Pontis, S.; Armirotti, A.; Cardinali, G.; Kovacs, D.; Migliore, M.; Summa, M.; Moreno-Sanz, G.; Picardo, M.; Piomelli, D. Endogenous *N*-acyl taurines regulate skin wound healing. *Proc. Natl. Acad. Sci. USA* **2016**, *113* (30), E4397–E4406.

43) Reiter, B.; Kraft, R.; Günzel, D.; Zeissig, S.; Schulzke, J.D.; Fromm, M.; Harteneck, C. TRPV4-mediated regulation of epithelial permeability. *FASEB J.* 2006, 20 (11), 1802–1812.

44) Yamamoto, A.; Taniguchi, T.; Rikyuu, K.; Tsuji, T.; Fujita, T.; Murakami, M.; Muranishi, S. Effects of various protease inhibitors on the intestinal absorption and degradation of insulin in rats. *Pharm. Res.* **1994**, *11* (10), 1496–1500.

45) Diehl, K.H.; Hull, R.; Morton, D.; Pfister, R.; Rabemampianina, Y.; Smith, D.; Vidal, J.M.; van de Vorstenbosch, C. A good practice guide to the administration of substances and removal of blood, including routes and volumes. *J. Appl. Toxicol.* **2001**, *21* (1), 15–23.

46) Zhang, J.; Jinnai, S.; Ikeda, R.; Wada, M.; Hayashida, S.; Nakashima, K. A simple HPLC-fluorescence method for quantitation of curcuminoids and its application to turmeric products. *Anal. Sci.* **2009**, *25* (3), 385–388.

47) Bistline, R.G. Jr.; Rothman, E.S.; Serota, S.; Stirton, A.J.; Wrigley, A.N. Surface active agents from isopropenyl esters: acylation of isethionic acid and n-methyltaurine. *J. Am. Oil Chem. Soc.* **1971**, *48* (11), 657–660.

48) Iga, K.; Ogawa, Y.; Yashiki, T.; Shimamoto, T. Estimation of drug absorption rates using a deconvolution method with nonequal sampling times. *J. Pharmacokinet. Biopharm.* **1986**, *14* (2), 213–225.

49) Kakemi, K.; Arita, T.; Muranishi, S. Absorption and excretion of drugs. XXVII. Effect of nonionic surface-active agents on rectal absorption of sulfonamides. *Chem. Pharm. Bull.* **1965**, *13* (8), 976–985.

50) Oberle, R.L.; Moore, T.J.; Krummel, D.A. Evaluation of mucosal damage of surfactants in rat jejunum and colon. *J. Pharmacol. Toxicol. Methods.* **1995**, *33* (2), 75–81.

51) Zhang, L.; Zhu, W.; Lin, Q.; Han, J.; Jiang, L.; Zhang, Y. Hydroxypropyl-β-cyclodextrin functionalized calcium carbonate microparticles as a potential carrier for enhancing oral delivery of water-insoluble drugs. *Int. J. Nanomedicine* **2015**, *10*, 3291–3302.

52) Soliman, O.A.E.; Mohamed, E.A.M.; El-Dahan, M.S.; Khatera, N.A.A. Potential use of cyclodextrin complexes for enhanced stability, anti-inflammatory efficacy, and ocular bioavailability of loteprednol etabonate. *AAPS PharmSciTech.* **2017**, *18* (4), 1228–1241.

53) Che, J.; Wu, Z.; Shao, W.; Guo, P.; Lin, Y.; Pan, W.; Zeng, W.; Zhang, G.; Wu, C.; Xu, Y. Synergetic skin targeting effect of hydroxypropyl-β-cyclodextrin combined with microemulsion for ketoconazole. *Eur. J. Pharm. Biopharm.* **2015**, *93*, 136–148.

54) Matilainen, L.; Toropainen, T.; Vihola, H.; Hirvonen, J.; Järvinen, T.; Jarho, P.; Järvinen, K. In vitro toxicity and permeation of cyclodextrins in Calu-3 cells. *J. Control. Release* **2008**, *126* (1), 10–16.

55) Doi, N.; Tomita, M.; Hayashi, M. Absorption enhancement effect of acylcarnitines through changes in tight junction protein in Caco-2 cell monolayers. *Drug Metab. Pharmacokinet.* **2011**, *26* (2), 162–170.

56) Fenyvesi, F.; Réti-Nagy, K.; Bacsó, Z.; Gutay-Tóth, Z.; Malanga, M.; Fenyvesi, É.; Szente, L.; Váradi, J.; Ujhelyi, Z.; Fehér, P.; Szabó, G.; Vecsernyés, M.; Bácskay, I. Fluorescently labeled methyl-beta-cyclodextrin enters intestinal epithelial Caco-2 cells by fluid-phase endocytosis., *PloS ONE* **2014**, *9* (1), e84856.

57) Maria, D.N.; Mishra, S.R.; Wang, L.; Abd-Elgawad, A.H.; Soliman, O.A.; El-Dahan, M.S.; Jablonski, M.M. Water-soluble complex of curcumin with cyclodextrins: Enhanced physical properties for ocular drug delivery. *Curr. Drug Deliv.* **2017**, *14* (6), 875–886.

58) Bradford, M.M. A rapid and sensitive method for the quantitation of microgram quantities of protein utilizing the principle of protein-dye binding. *Anal. Biochem.* **1976**, *72*, 248–254.

59) Gao, Y.; He, L.; Katsumi, H.; Sakane, T.; Fujita, T.; Yamamoto, A. Improvement of intestinal absorption of water-soluble macromolecules by various polyamines: intestinal mucosal toxicity and absorption-enhancing mechanism of spermine. *Int. J. Pharm.* **2008**, *354* (1-2), 126–134.

60) Capaldo, C.T.; Farkas, A.E.; Hilgarth, R.S.; Krug, S.M.; Wolf, M.F.; Benedik, J.K.; Fromm, M.; Koval, M.; Parkos, C.; Nusrat, A. Proinflammatory cytokine-induced tight junction remodeling through dynamic self-assembly of claudins. *Mol. Biol. Cell* **2014**, *25* (18), 2710–2719.

61) Vázquez, C.M.; Zanetti, R.; Ruiz-Gutierrez, V. Lipid composition and fluidity in the jejunal brush-border membrane of spontaneously hypertensive rats. Effects on activities of membrane-bound proteins. *Biosci. Rep.* **1996**, *16* (3), 217–226.

62) Saito, H.; Minamida, T.; Arimoto, I.; Handa, T.; Miyajima, K. Physical states of surface and core lipids in lipid emulsions and apolipoprotein binding to the emulsion surface. *J. Biol. Chem.* **1996**, *271* (26), 15515–15520.

63) Higuchi, T.; Connors, K.A. Phase solubility techniques. *Adv. Anal. Chem. Instrum.* **1965**, *4*, 117–122.

64) Loftsson, T.; Jarho, P.; Másson, M.; Järvinen, T. Cyclodextrins in drug delivery. *Expert Opin. Drug Deliv.* **2005**, *2* (2), 335–351.

65) Malanga, M.; Szemán, J.; Fenyvesi, É.; Puskás, I.; Csabai, K.; Gyémánt, G.; Fenyvesi, F.; Szente, L. "Back to the Future": A New Look at Hydroxypropyl Beta-Cyclodextrins. *J. Pharm. Sci.* **2016**, *105* (9), 2921–2931.

66) Salama, N.N.; Eddington, N.D.; Fasano, A. Tight junction modulation and its relationship to drug delivery. *Adv. Drug Deliv. Rev.* **2006**, *58* (1), 15–28.

67) Komuro, Y.; Ishihara, K.; Ohara, S.; Saigenji, K.; Hotta, K. Effects of tetragastrin on mucus glycoprotein in rat gastric mucosal protection. *Gastroenterol. Jpn.* **1992**, *27* (5), 597–603.

68) Kiss, T.; Fenyvesi, F.; Bácskay, I.; Váradi, J.; Fenyvesi, E.; Iványi, R.; Szente, L.; Tósaki, A.; Vecsernyés, M. Evaluation of the cytotoxicity of beta-cyclodextrin derivatives: evidence for the role of cholesterol extraction. *Eur. J. Pharm. Sci.* **2010**, *40* (4), 376–380.

69) Ohtani, Y.; Irie, T.; Uekama, K.; Fukunaga, K.; Pitha, J. Differential effects of alpha-, beta- and gamma-cyclodextrins on human erythrocytes. *Eur. J. Biochem.* **1989**, *186* (1-2), 17–22.

70) Róka, E.; Ujhelyi, Z.; Deli, M.; Bocsik, A.; Fenyvesi, É.; Szente, L.; Fenyvesi, F.; Vecsernyés, M.; Váradi, J.; Fehér, P.; Gesztelyi, R.; Félix, C.; Perret, F.; Bácskay, I.K. Evaluation of the cytotoxicity of α-cyclodextrin derivatives on the Caco-2 cell line and human erythrocytes. *Molecules* **2015**, *20* (11), 20268–20285.

71) Loftsson, T.; Brewster, M.E. Pharmaceutical applications of cyclodextrins: basic science and product development. *J. Pharm. Pharmacol.* **2010**, *62* (11), 1607–1621.

72) Reagan-Shaw, S.; Nihal, M.; Ahmad, N. Dose translation from animal to human studies revisited. *FASEB J.* **2008**, *22* (3), 659–661.

73) Zhao, H.; Lappalainen, P. A simple guide to biochemical approaches for analyzing protein-lipid interactions. *Mol. Biol. Cell.* **2012**, *23* (15), 2823–2830.

74) Maroni, A.; Zema, L.; Del Curto, M.D.; Foppoli, A.; Gazzaniga, A. Oral colon delivery of insulin with the aid of functional adjuvants. *Adv. Drug Deliv. Rev.* **2012**, *64* (6), 540–556.

Publications and presentations

Original articles:

- **Li, X.**; Kawamura, A.; Sato, Y.; Kusamori, K.; Katsumi, H.; Sakane, T.; Yamamoto, A. Improvement of the solubility and intestinal absorption of curcumin by *N*-Acyl taurates and elucidation of the absorption-enhancing mechanisms. *Biol. Pharm. Bull.* **2017**, *40* (12), 2175–2182.

- **Li, X.**; Uehara, S.; Sawangrat, K.; Morishita, M.; Kusamori, K.; Katsumi, H.; Sakane, T.; Yamamoto, A. Improvement of intestinal absorption of curcumin by cyclodextrins and the mechanisms underlying absorption enhancement. *Int. J. Pharm.* **2018**, *535* (1-2), 240–349.

Presentations:

- **李 鑫鵬**、草森浩輔、勝見英正、坂根稔康、山本 昌: Improvement of solubility and intestinal absorption of curcumin by various cyclodextrins. 日本薬剤学会第 30 年会 (長崎), 2015.5.
- **李 鑫鵬**、草森浩輔、勝見英正、坂根稔康、山本 昌: Improvement of solubility and intestinal absorption of curcumin by various cyclodextrins. 第 31 回日本 DDS 学会学術集会 (東京), 2015.7.
- **李 鑫鵬**、河村亜美、佐藤雄亮、草森浩輔、勝見英正、坂根稔康、山本 昌: Effects of *N*-acyl taurates on the solubility and intestinal absorption of curcumin. 日本薬剤学会第 31 年会 (岐阜), 2016.5.
- **李 鑫鵬**, 草森浩輔、勝見英正、坂根稔康、山本 昌: Absorption of curcumin from different administration routes and improvement of its nasal absorption by the co-administration with cyclodextrins. 第 32 回日本 DDS 学会学術集会 (静岡), 2016.7.